

Original article

UDC 550.84.092:553.411(575.1)

doi:10.52349/0869-7892_2025_102_117-138

Keywords: *association of pathfinder elements, gold ore mineralization, geochemical data processing, factor analysis, anomalous geochemical zones, mean deviation, standard deviation*

For citation: Oganiyozov B. B., Pirnazarov M. M. Geochemical halos of gold mineralization in the Geokhimicheskoe ore occurrence, Kuldzhuktau region (Uzbekistan). *Regional Geology and Metallogeny*. 2025; 32 (2): 117–138. https://doi.org/10.52349/0869-7892_2025_102_117-138

Научная статья

УДК 550.84.092:553.411(575.1)

doi:10.52349/0869-7892_2025_102_117-138

Ключевые слова: *ассоциация элементов-спутников, золоторудная минерализация, обработка геохимических данных, факторный анализ, выделение аномальных геохимических зон, среднее отклонение, стандартное отклонение*

Для цитирования: Оганиёзов Б. Б., Пирназаров М. М. Геохимические ореолы золотоносной минерализации участка Геохимическое гор Кульджуктау (Узбекистан) // Региональная геология и металлогения. 2025. Т. 32, № 2. С. 117–138. https://doi.org/10.52349/0869-7892_2025_102_117-138



© B. B. Oganiyozov,
M. M. Pirnazarov, 2025

Geochemical halos of gold mineralization in the Geokhimicheskoe ore occurrence, Kuldzhuktau region (Uzbekistan)

B. B. Oganiyozov✉, M. M. Pirnazarov

University of Geological Sciences, Tashkent, Uzbekistan,
behruzoga@gmail.com✉

Abstract. The Geokhimicheskoe ore occurrence is located 1–1.5 km west of the Tau-shan deposit, within the southeastern exocontact zone of the Aktosty intrusive massif. The study aims to comprehensively analyze geochemical halos associated with gold mineralization in the Kuldzhuktau region (Uzbekistan) in order to identify their spatial and compositional characteristics, establish indicator elements reflecting mineralization processes, and substantiate promising directions for precious metal prospecting. Factor analysis was applied to process multi-element geochemical data from 620 samples. The results demonstrate that average gold concentrations exceed background levels by up to 1,200 times; Au, As, Ag, and W are identified as key pathfinder elements. Additional ore-localizing features include “through-going” anomalies of As, W, Sb, Mo, and Ag. The constructed additive Au + As anomaly model proved to be most effective in delineating promising flanking and deep-seated zones. The established geochemical zoning, which reflects sequential formation of mineral assemblages, is confirmed as a critical criterion for predicting mineralization. The generated geochemical anomaly maps effectively highlight areas with high gold potential, providing guidance for further gold prospecting efforts.

Геохимические ореолы золотоносной минерализации участка Геохимическое гор Кульджуктау (Узбекистан)

Б. Б. Оганиёзов✉, М. М. Пирназаров

Университет геологических наук Республики Узбекистан,
Ташкент, Узбекистан, behruzoga@gmail.com✉

Аннотация. Рудопоявление Геохимическое расположено в 1,0–1,5 км к западу от месторождения Таушан в юго-восточной части экзоконтакта Актостинского интрузивного массива. Цель исследования — комплексное изучение геохимических ореолов, ассоциированных с золотоносной минерализацией на участке гор Кульджуктау (Узбекистан), для выявления их пространственно-вещественных особенностей, установления индикаторных элементов, отражающих минерализационные процессы, и обоснования перспективных направлений поисков благородных металлов. Для обработки многоэлементных данных 620 проб был применен факторный анализ. Установлено, что среднее содержание золота превышает фоновые значения до 1200 раз; элементами-индикаторами являются Au, As, Ag и W. Дополнительными рудолокализирующими признаками служат сквозные аномалии As, W, Sb, Mo и Ag. Созданная модель аномалии Au + As оказалась наиболее информативной для выделения перспективных фланговых и глубоких зон. Подтверждено, что геохимическая зональность, отражающая последовательность минерализационных процессов, является ключевым критерием прогнозирования оруденения. Построенные карты геохимических аномалий позволили локализовать зоны с высоким потенциалом, пригодные для дальнейших поисков золота.

INTRODUCTION

Geochemical methods are among the leading tools to explore various types of ore deposits [1]. Many deposits have been discovered when processing geochemical data and identifying anomalies [2]. Geochemical survey data include numerous elements. The complexity and diversity of geological processes lead to various elemental associations. Some of these associations are closely related to specific types of mineralization, which can be used to delineate promising ore-bearing positions [3]. Factor analysis is one of the most popular multivariate analysis methods employed to reduce data sets dimensionality. This tool combines several correlated variables into one factor in order to summarize multidimensional information [4]. In this regard, it recognizes geochemical associations related to specific types of mineralization.

Geochemical prospecting methods are used at the initial exploration stage to distinguish real anomalies from background values. Two different types of mathematical models have been developed to determine the threshold that effectively separates geochemical anomalies from background: (1) frequency-based and (2) spatial frequency-based. The first type relies on the frequency distribution of geochemical survey data. These include probability plots [5] and multivariate data analysis methods [6], which are often employed to analyze geochemical data [1; 7–9]. The second model type considers not only frequency but also spatial distribution of the data. The concept of fractals was introduced as an effective tool to identify various geochemical associations [10]. Geochemical survey data generally do not follow a normal distribution but show a tendency towards a lognormal distribution. Meanwhile, the distribution of trace elements and their enrichment exhibit multifractal characteristics. Fractal models include a concentration-area model, spectrum-area model, concentration-distance model, local singularity index, and concentration-volume model [11]. These approaches take into account both the frequency distributions of geochemical data and their spatial self-similar characteristics.

The Geokhimicheskoe ore occurrence is a key study object in the Kuldzhuktau mountain region, which has been investigated for over half a century. This research requires deep theoretical support to improve the search for hidden ore bodies in the mining zone periphery in order to expand deposit scales. Many studies in this area focus on the geology of gold-bearing occurrences, ore-controlling structures, sources of ore-forming materials, and processes of gold ore formation¹. Some studies suggest that the origin of these ore occurrences is associated with magmatic-hydrothermal processes and closely linked to magmatism². Nevertheless, methods for recognizing geological processes related to gold-forming mineralization and identifying geochemical anomalies remain critical tasks.

In the present study, factor analysis was used to process data on the concentrations of 22 chemical elements. The main objectives of the study were as follows:

- to identify elemental associations to be effective for gold ore prospecting;

- to study the genesis of mineralization by chemical element distribution zones;

- to delineate geochemical anomalies based on the factor analysis results in order to define target zones of ore formation in the study area periphery.

The Kuldzhuktau Mountains, as the modern tectonic structure suggests, represent an Alpine uplift of sublatitudinal extension. The core consists of the Paleozoic folded basement rocks, while the flanks are made up of the Mesozoic–Cenozoic platform cover deposits. The folded basement includes highly dislocated sedimentary and volcano-sedimentary rock complexes from the Middle Ordovician to the Middle–Upper Carboniferous, intruded by magmatic complexes of gabbro-diorite ($\lambda\delta P_1$) and granodiorite-granite ($\gamma\delta P_1$) composition³.

Terrigenous formations are the most widespread, constituting over two-thirds of the Paleozoic outcrop area. The oldest among them, lying at the base of the Paleozoic sequence, belong to the volcanogenic-terrigenous formation corresponding to the Kazakasu Formation ($O_{2-3}kz$)⁴, which has limited distribution. Rocks of this formation are predominantly located in the northern and eastern parts of the region, appearing as narrow bands of sublatitudinal orientation. They mainly comprise interbedded shales and sandstones with interlayers of siltstones, gravelites, conglomerates, siliceous rocks, and andesite-basalt volcanics [12].

Stratigraphic sequences, distribution, geological formations, folding age, and magmatism characteristics represent the Paleozoic formations of the Kuldzhuktau Mountains to the Zarafshan-Alai structural and formation zone situated in the southern part of the South Tien Shan folded system.

According to deep seismic sounding data, the modern Earth's crust thickness in the Kuldzhuktau area is approximately 40 km, with the granite-gneiss layer (18 km) being thinner than the basalt layer (22 km).

Due to intense compression, the geological formations are heavily deformed. The primary folded structure of the Paleozoic basement is the complexly built Kuldzhuktau synclinorium, stretching sublatitudinally for tens of kilometers. It is most clearly expressed in the eastern half of the mountains, where its core includes the Middle–Upper Carboniferous terrigenous and molasse deposits of the Taushan and Kamystin formations. These are the main host rocks for gold mineralization in the area. The synclinorium flanks are made up of the Lower Paleozoic terrigenous and carbonate rocks. Both the core and flanks are further complicated by numerous higher-order folds and fault zones [13].

¹Report on preliminary specialized prospecting for gold and other mineral resources within the Taushan Formation in the Central and Southeastern Kuldzhuktau Mountains, 2017–2020 / A. A. Kushiev [et al.]. Vol. IV. (In Russ.).

²Ibid.

³Ibid.

⁴Report on the geological structure and mineral resources of the K-41-115-A (southern), K-41-115-B (central and southern), and K-41-128-B (northern) sheet areas (report of the Kuldzhuktau geological survey party about the geological mapping results, scale of 1 : 50,000, 1967–1968 / Ya. B. Aysanov [et al.]. Vol. 1. Ore deposits of Uzbekistan: Monograph. Tashkent: IMR; 2001. (In Russ.).

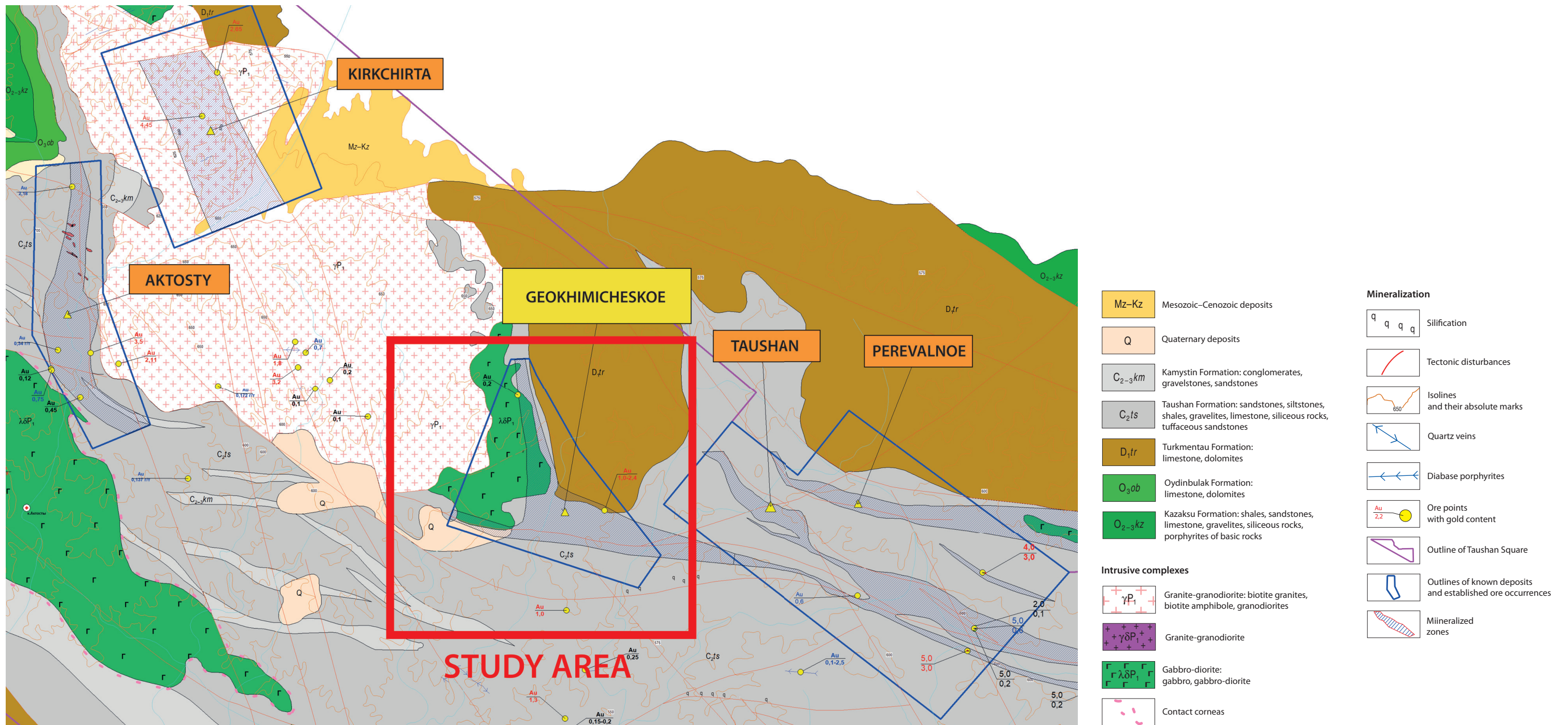


Fig. 1. Geological structure map of the promising Geokhimicheskoe ore occurrence

Source: from A. A. Kushiev [et al.]*

Рис. 1. Схема геологического строения перспективного рудопоявления Геохимическое

Источник: по А. А. Кушиеву [и др.]**

*Report on preliminary specialized prospecting for gold and other mineral resources within the Taushan Formation in the Central and Southeastern Kuldzhuktau Mountains, 2017–2020 / A. A. Kushiev [et al.]. Vol. IV. (In Russ.).

**Отчет по теме: «Опережающие специализированные поисковые работы на золото и другие полезные ископаемые в пределах развития таушанской свиты в центральной и юго-восточной части гор Кульджуктау» за 2017–2020 гг. / А. А. Кушиев [и др.]. Кн. IV.

Thrust structures¹ are accompanied by metasomatic alterations and control mineralization in the Aktosty (in the western exocontact of the Aktosty granite massif), South Sultanbibi (in the eastern exocontact of the Shaidaraz massif), and Adylsay occurrences (in the eastern exocontact of the Taushan massif). These fault zones should have a significant impact on the region's metallogeny. Fault zones are likely to play a vital role in the area's metallogeny.

According to the metallogenic zoning of Western Uzbekistan [14], the Kuldzhuktau region belongs to the Zarafshan-Gissar ore belt specializing in W, Sn, As, Mo, Sb, Pb, Zn, etc., and is part of the Zarafshan-Alay metallogenic zone [15]. It was recognized as a gold-tungsten-tin-antimony-mercury belt, later subdivided into several ore clusters and fields [16].

Exploration in the area led to discoveries of various mineral occurrences and prospects, such as:

- small occurrences of nickel, titanium, copper, cobalt in hyperbasites and gabbroids of the Shaidaraz and Taushan intrusives;

- contact-metasomatic formations linked to the Upper Carboniferous gabbro-diorite intrusions within the Beltau intrusive, associated with the large Taskazgan nickel-graphite deposit and several graphite, nickel, and copper occurrences in Shaidaraz and Taushan;

- hydrothermal gold and associated elements (Sb, As, Cu, W) mostly in terrigenous deposits of the Taushan Formation, less commonly in granitoids of the Aktosty and Tozbulak massifs;

- small hydrothermal mercury occurrences in the Middle Paleozoic carbonate sequences (Silurian and Devonian) [12].

Among all the known mineral resources of Kuldzhuktau, only graphite, nickel, and gold are currently of industrial interest. Fifteen antimony-mercury-type ore occurrences² have been identified, but they are too small to be cost-effective for now.

Non-metallic resources include:

- quartz deposit (Tozbulak);
- granite deposit;
- several marble deposits;
- occurrences of phosphorus, wollastonite, brucite, Iceland spar, magnesite, zeolites, bentonite clays;
- occurrences of turquoise, opal, and onyx.

Most gold occurrences in Kuldzhuktau are endogenous and belong to the gold-quartz-sulfide formation. These include:

- deposits: Taushan, Yangikazgan;
- occurrences: Tsentralnoe, Kirkchirta, Aktosty, Perevalnoe, Adylsay, Dzhurakuduk, Shaidaraz, Taskazgan, Darvaza, etc.

Most of them are located in the sandy-shale deposits of the Lower Taushan Formation (C₂t_s), often

where they contact carbonate-siliceous rocks. Two occurrences — Kirkchirta and Tsentralnoe — are in granitoids, and one — Darvaza — is in sandstones and shales of the Kazakasu Formation.

Kuldzhuktau is among the least-studied mountain areas in the Central Kyzylkum region. Systematic exploration was conducted until the mid-1980s and resumed in 2016. Since then, infrastructure has improved (e.g. construction of the new Kogan railway), and comprehensive exploration has restarted to expand the region's mineral base. Currently, further exploration is underway for deeper levels and flanks of the previously discovered Taushan and Yangikazgan gold deposits. The known occurrences, such as Perevalnoe, Aktosty, Kirkchirta, Adylsay, and Geokhimicheskoe, are being studied in more detail (fig. 1).

The Geokhimicheskoe ore occurrence lies 1–1.5 km west of the Taushan deposit, in the southeastern exocontact of the Aktosty intrusive massif. It is located at the intersection of a submeridional arc-shaped thrust fault and steeply dipping faults of sublatitudinal orientation, which are part of or associated with the Sultanbibi fault zone. The central, southern, and eastern parts of the area are composed of sandstones and siliceous rocks of the Taushan Formation. The Devonian limestone occurs in the north, and gabbro-diorites of the Aktosty massif are found in the west.

The area clearly shows faults in three directions: sublatitudinal northwestern (longitudinal), submeridional (transverse thrust type), and sublatitudinal northeastern (fig. 2).

MATERIAL AND METHODS

Mineralogical and petrographic characteristics of the main rock types in the Geokhimicheskoe ore occurrence

In the Geokhimicheskoe ore occurrence, metamorphosed sedimentary-terrigenous, intrusive, effusive formations, and their metasomatically altered varieties have been identified. Quartz vein formations are also frequently observed. The intrusive formations are represented by granitoids, while the effusive rocks include diorites and dacites. Below is a description of the main rock types. Fig. 3 demonstrates the samples locations.

1. Metamorphosed sedimentary-terrigenous rocks. These rocks are primarily composed of metamorphosed sandstones, shales, and siltstones, which have undergone varying degrees of regional and contact metamorphism. The mineral composition includes quartz, feldspar, mica (muscovite and biotite), and chlorite. The rocks often exhibit foliation and schistosity, with secondary minerals, such as sericite and epidote, developed. These formations are commonly crosscut by quartz veins and veinlets, which relate to gold mineralization.

2. Intrusive rocks (granitoids). The granitoids in the Geokhimicheskoe ore occurrence are characterized by a medium- to coarse-grained texture. The primary mineral assemblage includes quartz, plagioclase, potassium feldspar, and biotite. Accessory minerals contain zircon, apatite, and opaque minerals of magnetite and

¹Report on the geological structure and mineral resources of the K-41-115-A (southern), K-41-115-B (central and southern), and K-41-128-B (northern) sheet areas (report of the Kuldzhuktau geological survey party about the geological mapping results, scale of 1 : 50,000, 1967–1968 / Ya. B. Aysanov [et al.]. Vol. 1. Ore deposits of Uzbekistan: Monograph. Tashkent: IMR; 2001. (In Russ.).

²Finkelstein Yu. V. Report on revision and evaluation, revision and exploration work in the Kuldzhuktau Mountains in 1968–1969, 1971 / Yu. V. Finkelstein [et al.]. Zarafshan.

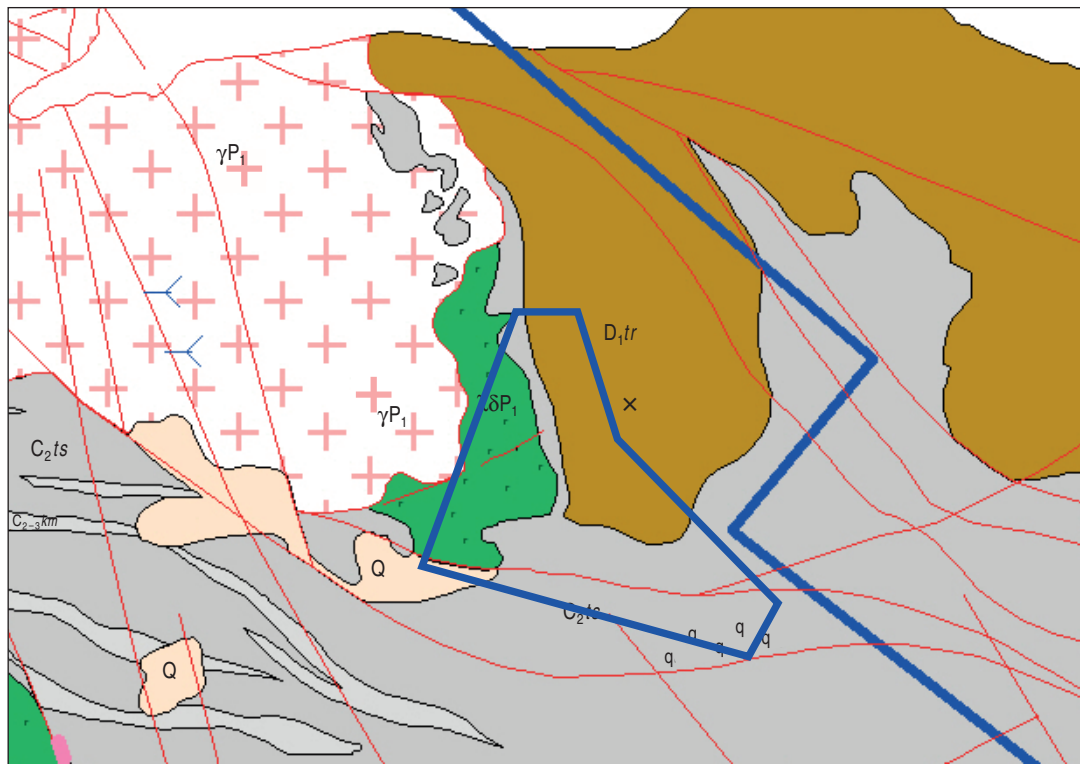
ilmenite. The granitoids often exhibit hydrothermal alteration, with secondary minerals, such as sericite, chlorite, and epidote, developed. These rocks frequently attribute to quartz-sulfide veins, which host gold mineralization.

3. Effusive rocks (diorites and dacites). The effusive rocks are represented by diorites and dacites, which exhibit porphyritic textures. The diorites are mainly composed of plagioclase, amphibole, and pyroxene, while the dacites contain plagioclase, quartz, and biotite. These rocks often demonstrate signs of hydrothermal alteration, with secondary minerals of chlorite, epidote, and sericite developed. The effusive rocks are crosscut by quartz veins and attribute to zones of gold mineralization.

4. Metasomatically altered rocks. Metasomatic alteration is widespread in the Geokhimicheskoe ore occurrence

and is closely associated with gold mineralization. The altered rocks are characterized by the development of sericite, quartz, carbonates, and sulfides. Pyrite, arsenopyrite, and chalcopyrite are the most common sulfide minerals, often occurring as disseminated grains or in veinlets. The alteration zones typically relate to fault and shear zones, which acted as conduits for hydrothermal fluids.

5. Quartz vein formations. Quartz veins are a prominent feature of the Geokhimicheskoe ore occurrence and are the primary host for gold mineralization. The veins range in thickness from a few millimeters to several meters and often attribute to sulfide minerals. The quartz is typically milky to translucent and may contain visible gold in some cases. The veins are often surrounded by alteration halos, characterized by sericitization, silicification, and sulfidation.



Conventional designations

	Plot outline		Kamystin Formation: conglomerates
	Tectonic faults		Taushan Formation: sandstones, siltstones

Fig. 2. Faults in the Geokhimicheskoe ore occurrence

Source: from A. A. Kushiev*

Рис. 2. Разрывные нарушения рудопроявления Геохимическое

Источник: по А. А. Кушиеву**

*Report on preliminary specialized prospecting for gold and other mineral resources within the Taushan Formation in the Central and Southeastern Kuldzhuktau Mountains, 2017–2020 / A. A. Kushiev [et al.]. Vol. IV. (In Russ.).

**Отчет по теме: «Опережающие специализированные поисковые работы на золото и другие полезные ископаемые в пределах развития таушанской свиты в центральной и юго-восточной части гор Кульджуктау» за 2017–2020 гг. / А. А. Кушиев [и др.]. Кн. IV.

In summary, a complex assemblage of metamorphosed sedimentary-terrigenous rocks, intrusive granitoids, effusive diorites and dacites, and their metasomatically altered varieties characterizes the Geokhimicheskoe ore occurrence. Quartz vein formations are widespread and play a key role in gold mineralization. The mineralogical and petrographic characteristics of these rocks provide important insights into the processes of ore formation and the structural controls of mineralization. Fig. 3 illustrates the studied samples locations.

The rock is a brown-colored quartz-sericite breccia with a granoblastic to lepidogranoblastic structure and a brecciated texture (figs. 4, 5). It consists of angular fragments of sericite-quartz schist (1–7 mm in size) and quartzite (up to 4.2 mm) cemented by vein-like and nodular carbonate aggregates. The schist fragments are composed of polygonal, elongated quartz grains (up to 0.15 mm long) with evenly distributed sericite flakes (up to 0.12 mm). The cementing matrix contains carbonate grains (transparent calcite and ferruginous carbonate) up to 0.65 mm in size, with many ferruginous carbonate grains showing zonal distribution of fine iron hydroxide particles. The mineral composition is quartz (60–80 %), carbonate (15–40 %), and sericite (0.5–5 %).

Quartzite with sericite and schistose, with recrystallization veins, weakly limonitized. The rock has a lepidogranoblastic structure and a poorly defined schistose texture. It is composed of polygonal-isometric and elongated quartz grains, approximately 0.05 mm in size, among which thin, elongated sericite flakes are

almost uniformly distributed and oriented in one direction. In thin sections, “washed-out” areas are observed, consisting of sericite aggregates with thin veins of carbonaceous material.

Recrystallization veins and nests contain polygonal quartz grains, some of which exhibit transverse columnar grains ranging from 0.07 to 0.75 mm in length (fig. 6). The mineral composition of the rock is as follows: quartz 85–90 %, sericite 7–10 %, iron hydroxides 1–2 %, carbonaceous material 1–2 %.

Pseudomorphs of iron hydroxides. Pseudomorphs of iron hydroxides are unevenly distributed in the rock. Their form is polygonal, often corresponding to a cubic habit.

Uneven-grained sandstone. The rock exhibits a breccia-like texture. The clastic grains contain fine polygonal quartz grains. The cement is of carbonate-sericite composition (fig. 7). Sericite flakes, which present vein-like and streaky accumulations of finely flaked sericite, are oriented in one direction. Aggregates of ferruginous carbonate have a sharply elongated form and are also aligned in the same direction as the sericite veins. Some aggregates consist of irregular calcite grains and polygonal zonal grains of ferruginous carbonate. Iron hydroxides develop along the ferruginous carbonate, often forming small nodular segregations up to 0.1–0.2 mm in size.

In porphyritic varieties of dacites, the porphyritic segregations are represented by irregular polygonal quartz grains up to 1.5 mm in size. The mineral composition of the rock is as follows: quartz 55–60 %,

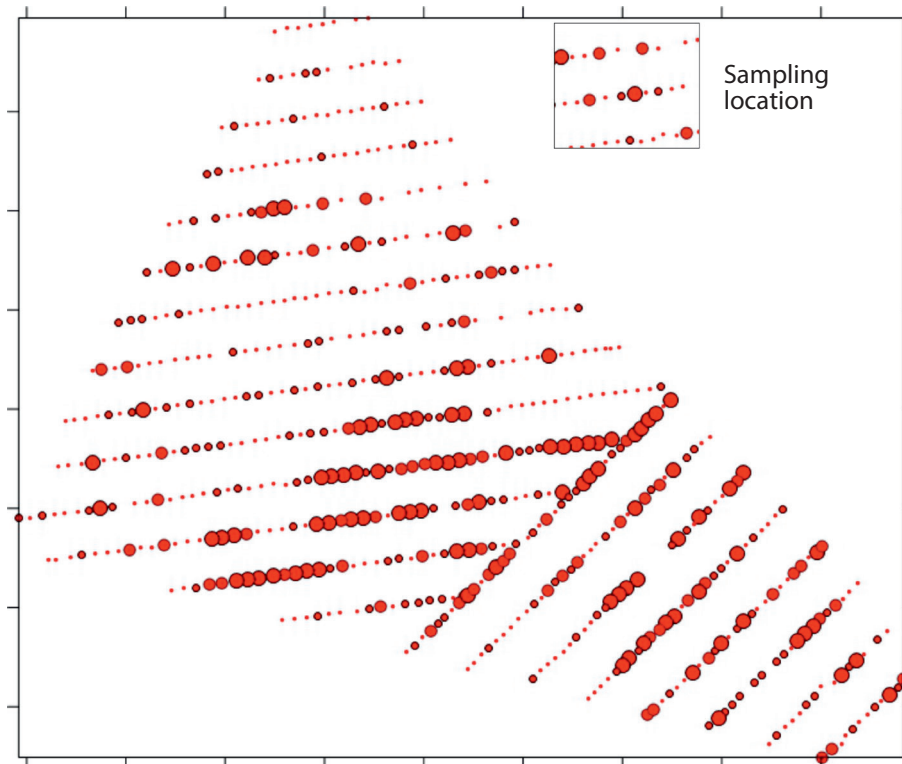


Fig. 3. Sampling locations from the Geokhimicheskoe ore occurrence

Рис. 3. Места отбора изученных проб из рудопоявления Геохимическое

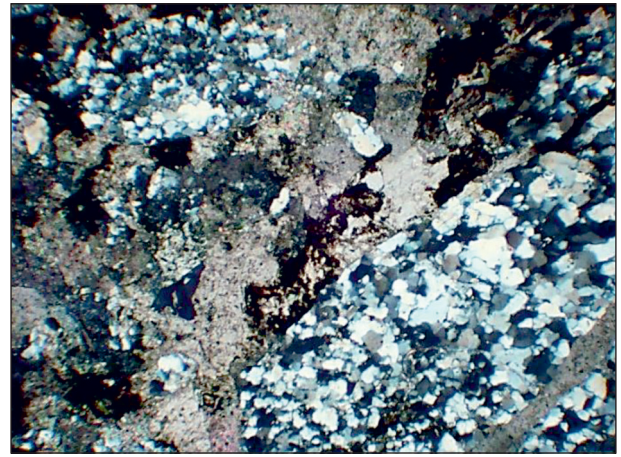
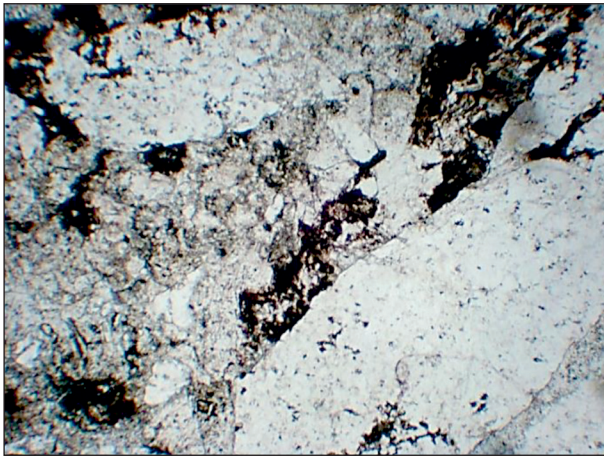


Fig 4. Breccia of sericite-quartz schist. Thin section Sb-8. Magnification 32x; nicoli + and li

Рис. 4. Брекчия серицит-кварцевого сланца. Шлиф Sb-8. Увелич. 32x; николи + и li

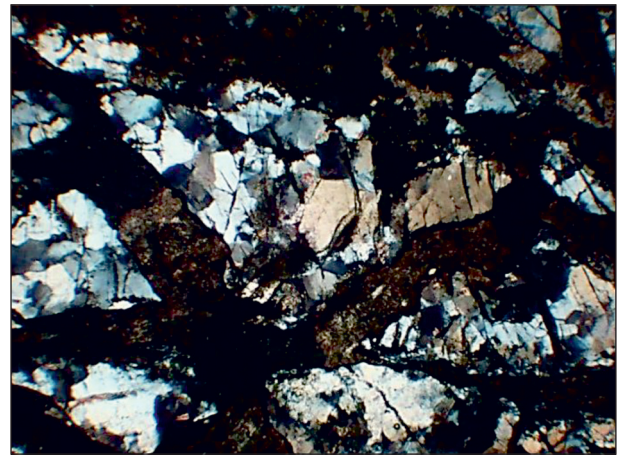
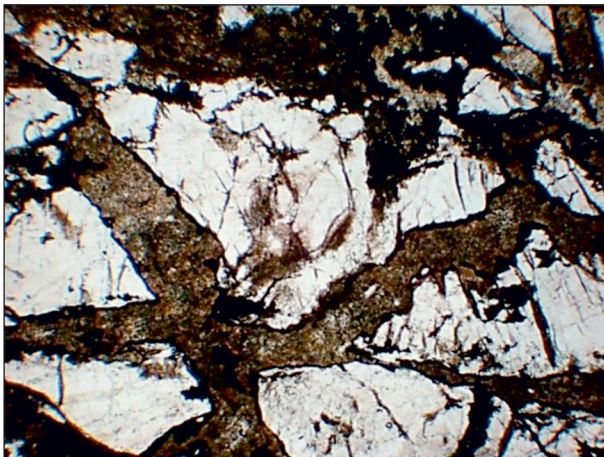


Fig. 5. Quartzite breccia cemented by fibrous iron carbonate precipitates. Thin section Sb-9. Magnification 32x; nicoli + and li

Рис. 5. Брекчия кварцита, сцементированная жилковатыми выделениями железистого карбоната. Шлиф Sb-9. Увелич. 32x; николи + и li

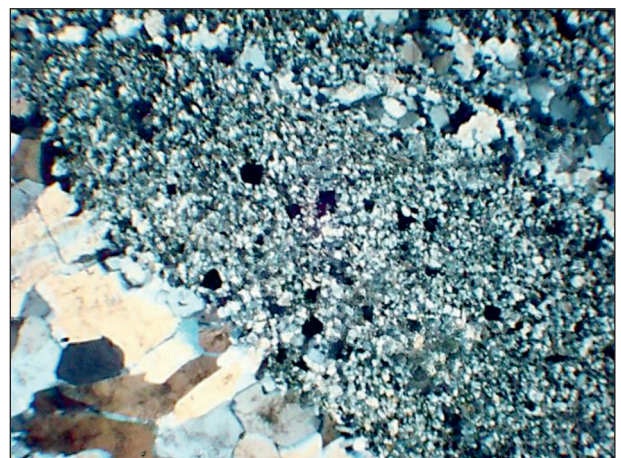
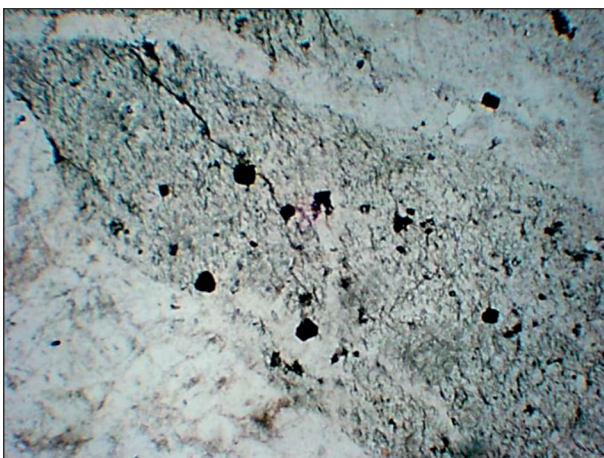


Fig. 6. Veins and nests of recrystallized quartz in quartzite. Thin section Sb-1. Magnification 32x; nicoli + and li

Рис. 6. Пржилки и гнезда перекристаллизованного кварца в кварците. Шлиф Sb-1. Увелич. 32x; николи + и li

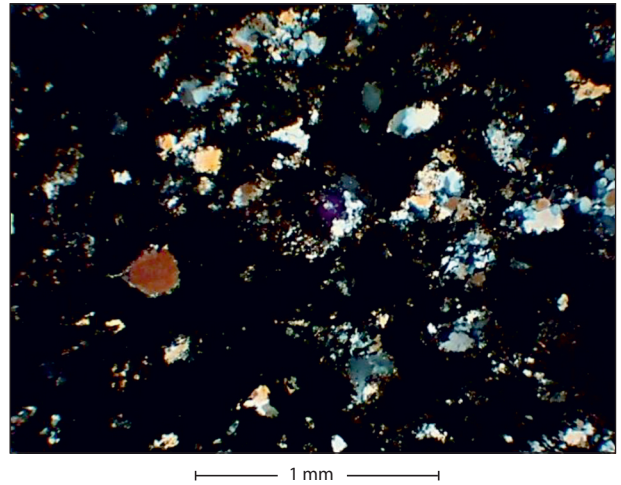
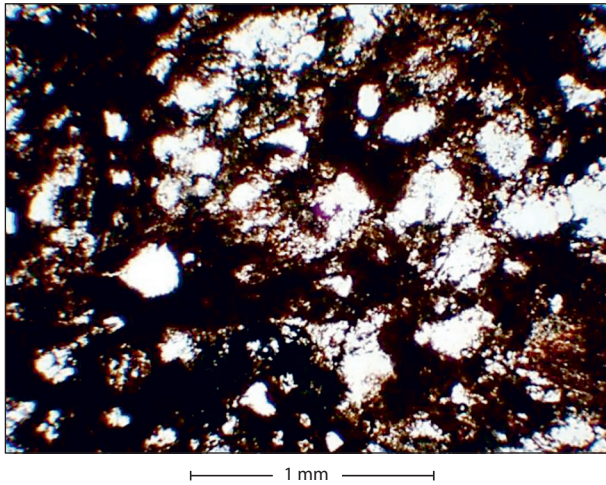


Fig. 7. Sandstone of sericite-quartz-carbonate composition. Thin section Sb-4. Magnification 32x; nicoli + and II
 Рис. 7. Песчаник серицит-кварц-карбонатного состава. Шлиф Sb-4. Увелич. 32x; николи + и II

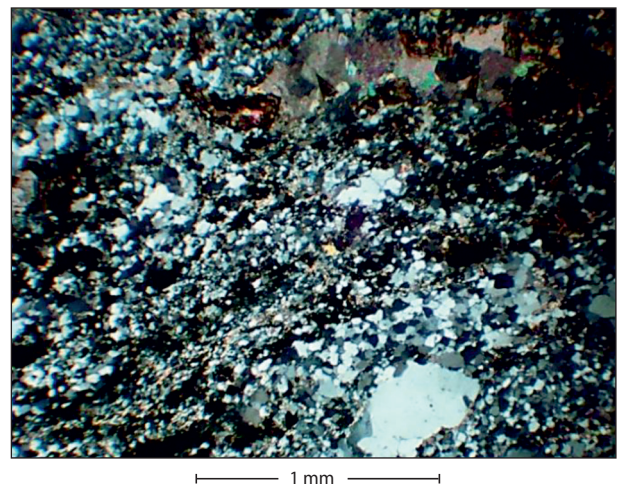
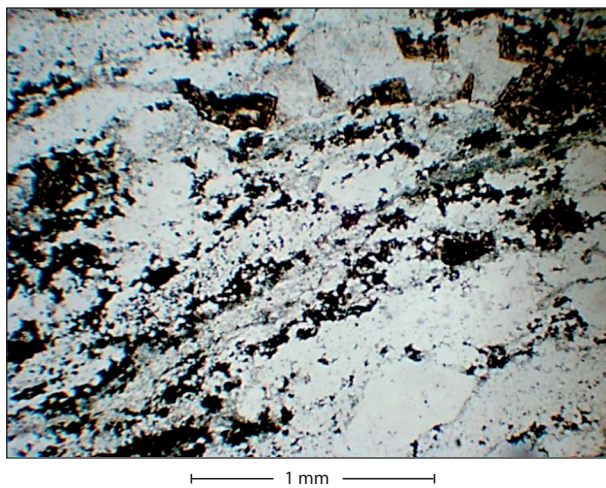


Fig. 8. Carbonate-sericite-quartz schist. Thin section Sb-5. Magnification 32x; nicoli + and II
 Рис. 8. Сланец карбонат-серицит-кварцевый. Шлиф Sb-5. Увелич. 32x; николи + и II

ferruginous carbonate 35–40 %, iron hydroxides 3–5 %, sericite 1–2 %, apatite 0.1 %. The rock is strongly carbonatized and iron-enriched, primarily in the form of ferruginous carbonate.

Carbonate-sericite-quartz schists (Sb-5, fig. 8), *sericite-quartz schists* (Sb-15), and *carbonate-quartz schists* (Sb-2, fig. 9). The rocks exhibit a lepidogranoblastic structure and schistose texture. The main mass of the rock is composed of fine polygonal quartz grains with unevenly distributed sericite flakes. Among these, vein-like and streaky accumulations of finely flaked sericite, oriented in one direction, are frequently observed. Aggregates of ferruginous carbonate have a sharply elongated form and are also aligned in the same direction as the sericite veins. Some aggregates consist of irregular calcite grains and polygonal zonal grains of ferruginous carbonate. The size of quartz grains ranges from 0.01 to 0.15 mm, while carbonate grains reach up to 0.2 mm.

The mineral composition of the schist is as follows: quartz 80–85 %, ferruginous carbonate 7–10 %, sericite

5–7 %, calcite 0.7–1 %. In the carbonate-quartz schists (Sb-2), banded distributions of microgranular carbonate aggregates and carbonaceous material are observed within the quartz mass, along with occasional sericite aggregates (fig. 9). The volumetric mineral composition of the rock is as follows: quartz 80–85 %, carbonate 10–15 %, carbonaceous material 2–3 %, sericite 0.5–1 %. The rock demonstrates signs of iron enrichment. Many carbonate aggregates are saturated with finely dispersed particles of iron hydroxides, which sometimes exhibit zonal distribution.

Medium-grained diorite, cataclastic, intensely margaritized, quartzified, chloritized, and muscovitized. The rock has a breccia-like texture (fig. 10). The rock is a diorite in which plagioclase has undergone intense margaritization (based on optical characteristics — higher refractive index and lower birefringence than sericite). In some grains of margaritized plagioclase, distinct twinning is preserved. The rock is cataclastic, and the newly formed quartz aggregates were likely to fill the

resulting voids. Grains of biotite are present in the rock, often completely replaced by chlorite and muscovite, with leucoxene formed along cleavage cracks and grain boundaries. The size of the former biotite grains reaches up to 0.3 mm.

Ilmenite forms sinuous, vein-like accumulations of micrograins and larger nodular grains up to 0.25 mm in size. The mineral composition of the rock is as follows: margarite 60–65 %, quartz 15–20 %, plagioclase 3–5 %, chlorite 3–5 %, muscovite 2–3 %, carbonate 1–2 %, ilmenite 0.5–1 %, biotite 0.5–0.7 %.

Quartz vein with sericite and carbonaceous material. The rock exhibits a lepidogranoblastic structure and massive texture (fig. 11). The rock consists of irregular polygonal quartz grains up to 0.3 mm in size and a small number of flakes of nearly isotropic chlorite. The quartz grains often have sharply angular shapes, with the largest grains frequently displaying sinuous boundaries.

Within the quartz mass, small sinuous vein-like accumulations of finely flaked carbonaceous material are observed, creating a schistose and layered texture in the rock. Occasionally, thin veins of iron hydroxides, approximately 0.025 mm in thickness, are present in the rock, along with pseudomorphs of iron hydroxides after pyrite, reaching up to 0.15 mm in size. The mineral composition of the rock is as follows: quartz 88–90 %, chlorite 3–4 %, carbonaceous material 2–3 %, iron hydroxides 2–3 %.

The studied rocks have undergone metasomatic alterations of varying degrees. The most widely observed alterations in the studied rocks include sericitization, silicification (quartzification), iron enrichment (ferruginization), and carbonatization. Ore mineralization is accompanied by intense carbonatization and silicification of the rocks. In some rocks, ferruginous carbonates are closely associated with iron hydroxides.

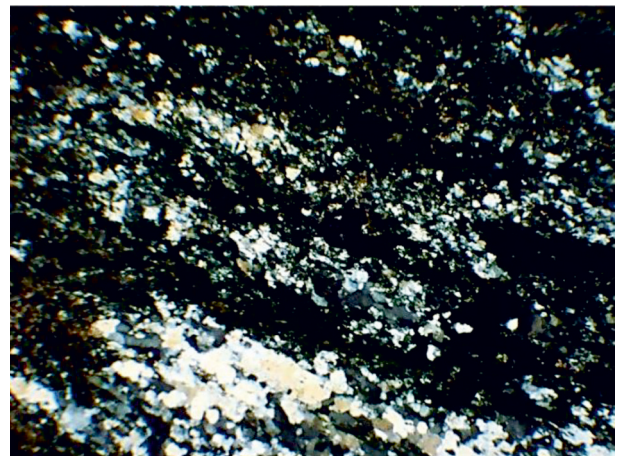
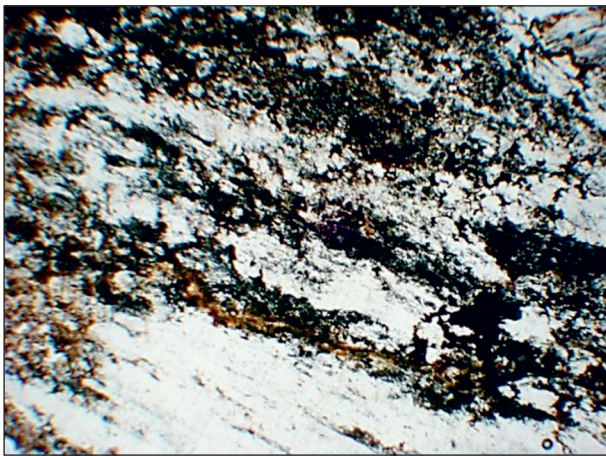


Fig. 9. Carbonate-quartz schist. Thin section Sb-2. Magnification 32 \times ; nicoli + and II

Рис. 9. Карбонат-кварцевый сланец. Шлиф Sb-2. Увелич. 32 \times ; николи + и II

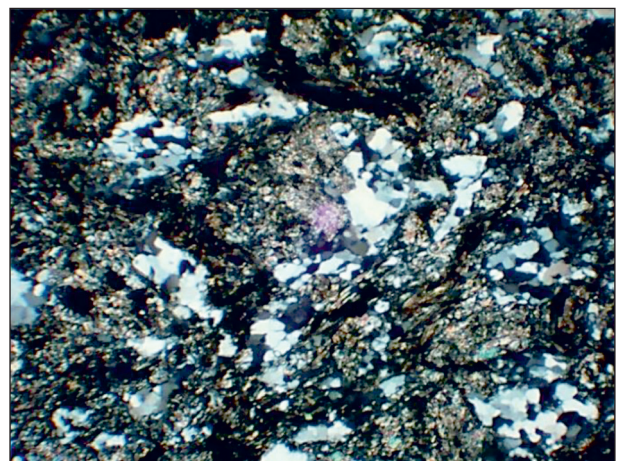
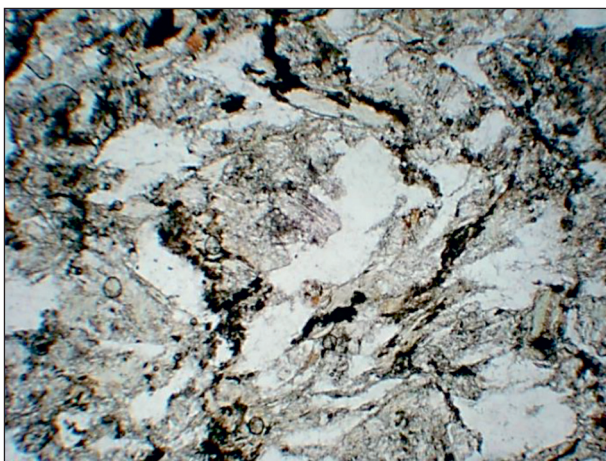


Fig. 10. Microscopic view of diorite in transmitted light. Thin section Sb-12. Magnification 32 \times ; nicoli + and II

Рис. 10. Микроскопический вид диорита в проходящем свете. Шлиф Sb-12. Увелич. 32 \times ; николи + и II

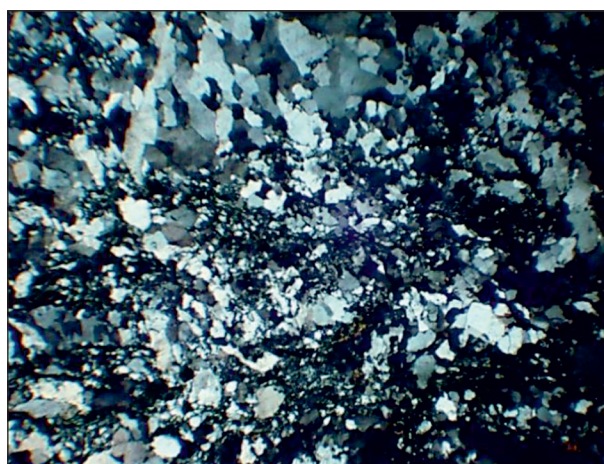
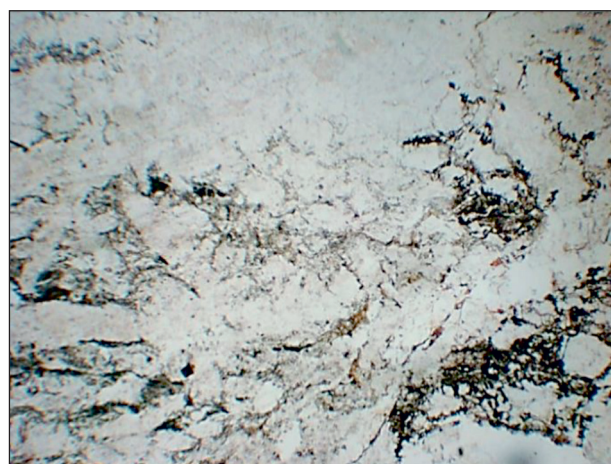


Fig. 11. Quartz vein. Thin section Sb-18. Magnification 32x; nicoli + and II

Рис. 11. Кварцевая жила. Шлиф Sb-18. Увелич. 32x; николи + и II

Since all the studied samples were collected from the surface (oxidation zone), the ore minerals are primarily represented by hydroxides, sulfates, and carbonates of iron. Ore minerals are mainly observed as individual disseminations, less frequently as thin veinlets, and as ochreous accumulations along rock fractures.

Data and sample collection

The study is based on a comprehensive geochemical dataset obtained from 620 samples systematically collected across the Geokhimicheskoe ore occurrence, covering an area of approximately 1.3 km². Sampling was conducted along geochemical traverses oriented perpendicular to three principal ore-controlling structures, and differential GPS equipment, which provides positional accuracy within 3 meters, precisely recorded the samples locations. The collected samples demonstrate the full lithological diversity of the area, including siltstones, shales, sandstones, diorites, granodiorites, limestone, and quartz veins. The channel sampling method, with each 400–600-gram composite sample representing a single lithological unit, contributed to uniform sampling. Prior to analysis, the samples underwent rigorous preparation including drying, crushing, washing, homogenization, and splitting in the certified laboratory of JSC “Uzbekgeologorazvedka” under the Ministry of Mining Industry and Geology of the Republic of Uzbekistan. Each sample was analyzed for a suite of 22 elements comprising Au, Ag, Cu, Pb, Zn, Ni, Co, As, Sb, Bi, Mo, W, Sn, Li, Be, Ga, Ge, Cd, Cr, V, Mn, and P, which provided complete geochemical characteristics of the ore occurrence. The analytical results form a robust dataset for understanding the mineralization patterns and exploration potential of the area.

Factor analysis

Factor analysis represents a robust statistical approach widely employed in geochemical data inter-

pretation. C. Reimann, P. Filzmoser, and R. G. Garrett [12] established its foundational principles. This dimensionality reduction technique effectively transforms complex multivariate datasets into a more manageable set of latent factors that capture essential patterns within the original variables [17; 18]. The methodology's strength lies in its ability to elucidate underlying geological processes rather than merely describing surface-level correlations¹. The mathematical framework of factor analysis follows a well-defined model where observed variables (y) are expressed as linear combinations of latent factors (f) through a loading matrix (Λ), with an additional error term (e) accounting for unique variances, as demonstrated in the fundamental equations $y = \Lambda f + e$ and $\text{Cov}(y) = \Lambda \Lambda^T + \Psi$ [9]. The diagonal matrix Ψ specifically contains these unique variances that cannot be explained by common factors [4]. In practical geological applications, this technique has proven invaluable for investigating ore formation mechanisms, characterizing mineralization processes and developing predictive models for concealed mineral deposits [12]. The analytical workflow typically involves visual interpretation of scree plots to determine optimal factor retention, examination of factor loading patterns to understand variable groupings, and spatial analysis through factor score mapping² [19; 20]. Prior to analysis, rigorous data preparation steps are essential, including appropriate data transformations (commonly logarithmic) and normality assessments complemented by diagnostic tests, such as the Kaiser-Meyer-Olkin measure for sampling adequacy and Bartlett's test of sphericity, to verify how suitable the correlation structure for factor analysis is [21]. Modern computational implementations, including specialized software packages such as STATISTICA

¹Borodachev S. M. Multidimensional statistical methods: Manual. Ekaterinburg: USTU — UPI; 2009. 81 p. (In Russ.).

²Factor analysis in geology: Manual for lab. classes / A. I. Bakhtin [et al.]. Kazan: Kazan State Univ.; 2007. 32 p.

(Version 10, StatSoft Inc.), facilitate efficient execution of these analytical procedures while ensuring methodological rigor in geochemical investigations. The comprehensive references supporting this discussion span foundational works through contemporary applications [12], collectively demonstrating the enduring relevance and evolving methodology of factor analysis in geochemical research.

RESULTS AND DISCUSSION

Statistical analysis

This study incorporated a comprehensive descriptive statistical analysis of chemical element concentrations, with key statistical parameters (mean values (MEAN) and standard deviations (STD DEV)) and average background levels for the Geokhimicheskoe ore occurrence presented in Table 1. The variation coefficient (CV) was employed to illustrate data dispersion patterns. The Clarke concentration value for gold reached 1266.67 ng/t, substantially exceeding typical upper crustal background levels in the Geokhimi-

cheskoe area. Both Au and As demonstrated variation coefficients approaching or exceeding 5, indicating pronounced spatial heterogeneity in their distribution and suggesting potential accumulation patterns near mineralized zones. Quantile-quantile plots served as an effective visualization tool for assessing element distribution characteristics [2]. The generated quantile-quantile plots (fig. 12) revealed that even after logarithmic transformation, the geochemical datasets failed to conform to normal distribution patterns, highlighting the complex nature of element dispersion in the study area. The statistical findings collectively suggest significant mineralization processes affecting Au and As distribution, with their anomalous concentrations potentially serving as important exploration indicators within the Geokhimicheskoe mineral system. The non-normal distribution patterns observed through quantile-quantile analysis further emphasize the need for specialized statistical approaches when interpreting such geochemical datasets, particularly when dealing with pathfinder elements exhibiting strong mineralization affinity. These analytical outcomes provide crucial baseline data for subsequent

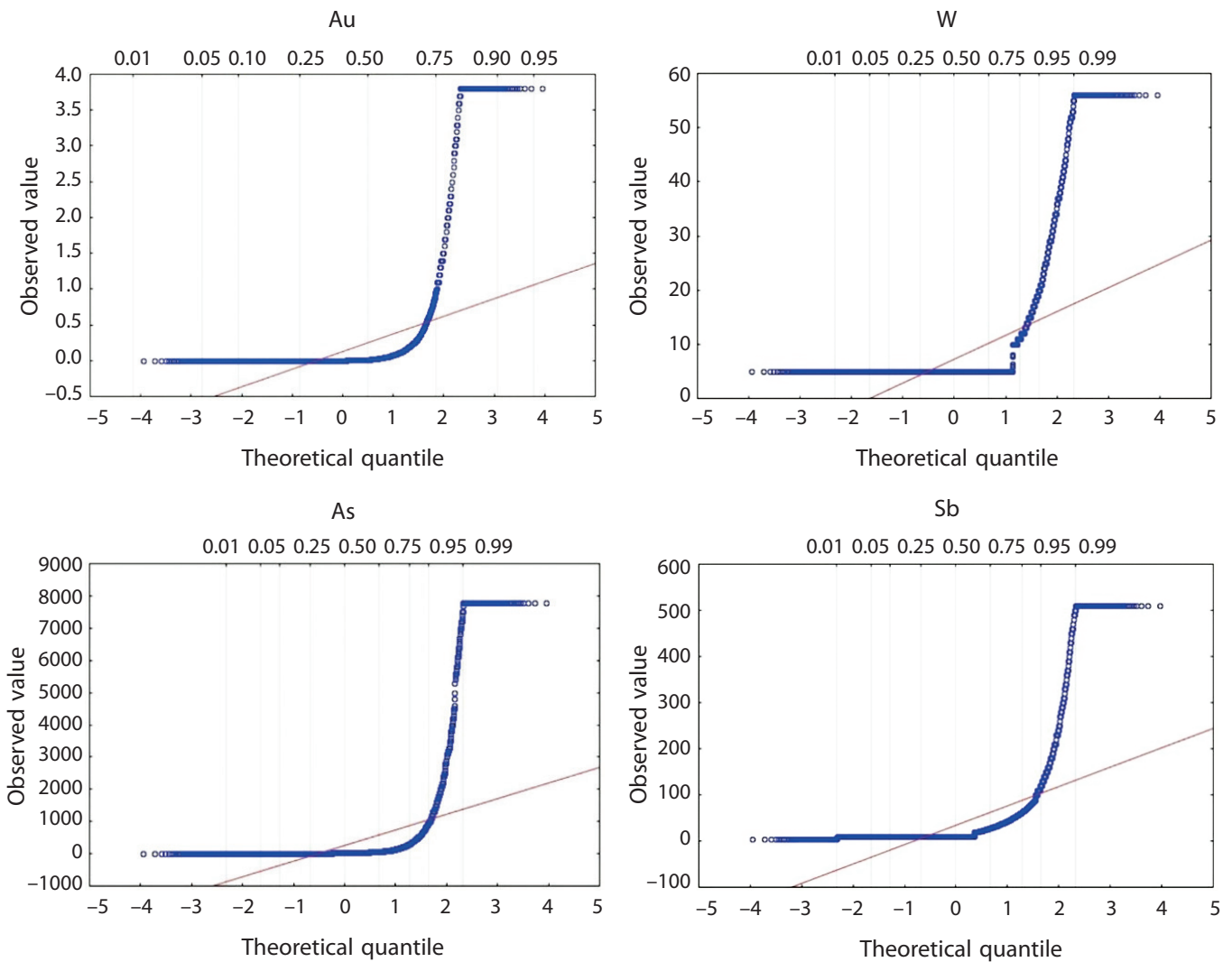


Fig. 12. Quantile-quantile plots of logarithmically transformed data for major elements in the section

factor analysis and spatial interpretation of element associations in the studied mineralization context.

Fig. 12 presents quantile-quantile plots illustrating distribution of observed concentrations of the chemical elements Au, W, As, Sb, Zn, Pb, Co, and Mo compared to the theoretical normal distribution. All the elements show significant deviation from normality, evident from the upward bending of data points in the upper quantiles. This pattern is especially pronounced for As, Sb, Zn, and W, where most data are clustered at lower values, followed by a sharp increase starting from approximately the 0.90–0.95 quantile range. This indicates the presence of anomalously high concentrations, typical of enrichment zones. The distribution of Au demonstrates a similar trend: the majority of points lie below the reference line, with a steep rise in the upper quantiles, suggesting local ore occurrences. Pb and Co exhibit more gradual deviations, although they also represent noticeable increases in higher quantiles. Mo stands out with a sharp and step-like rise in the upper range, pointing to isolated high concentrations against a generally low background. Overall, the distributions of all the examined elements

demonstrate positive skewness and anomalous values in the upper quantiles, indicating geochemical heterogeneity and the possible presence of mineralized zones within the study area.

The data points aligned along the central trend line represent dominant background concentrations within the geochemical dataset, while the values plotted at the both graph extremities correspond to relatively rare but geochemically significant anomalies that warrant particular attention. The investigation additionally examined element distribution patterns across different lithological units to evaluate host rock influences on metal enrichment. As detailed in Table 1, maximum gold concentrations were recorded in sandstone formations, whereas arsenic demonstrated peak values in siliceous siltstones followed by limestone sequences. Antimony exhibited its highest concentrations in quartz vein systems, with secondary enrichment in carbonate rocks found. Among siderophile elements, copper and cobalt demonstrated preferential accumulation in limestone lithologies, with subordinate concentrations occurred in quartz vein networks. These lithogeochemical patterns reveal distinct element-specific affinities

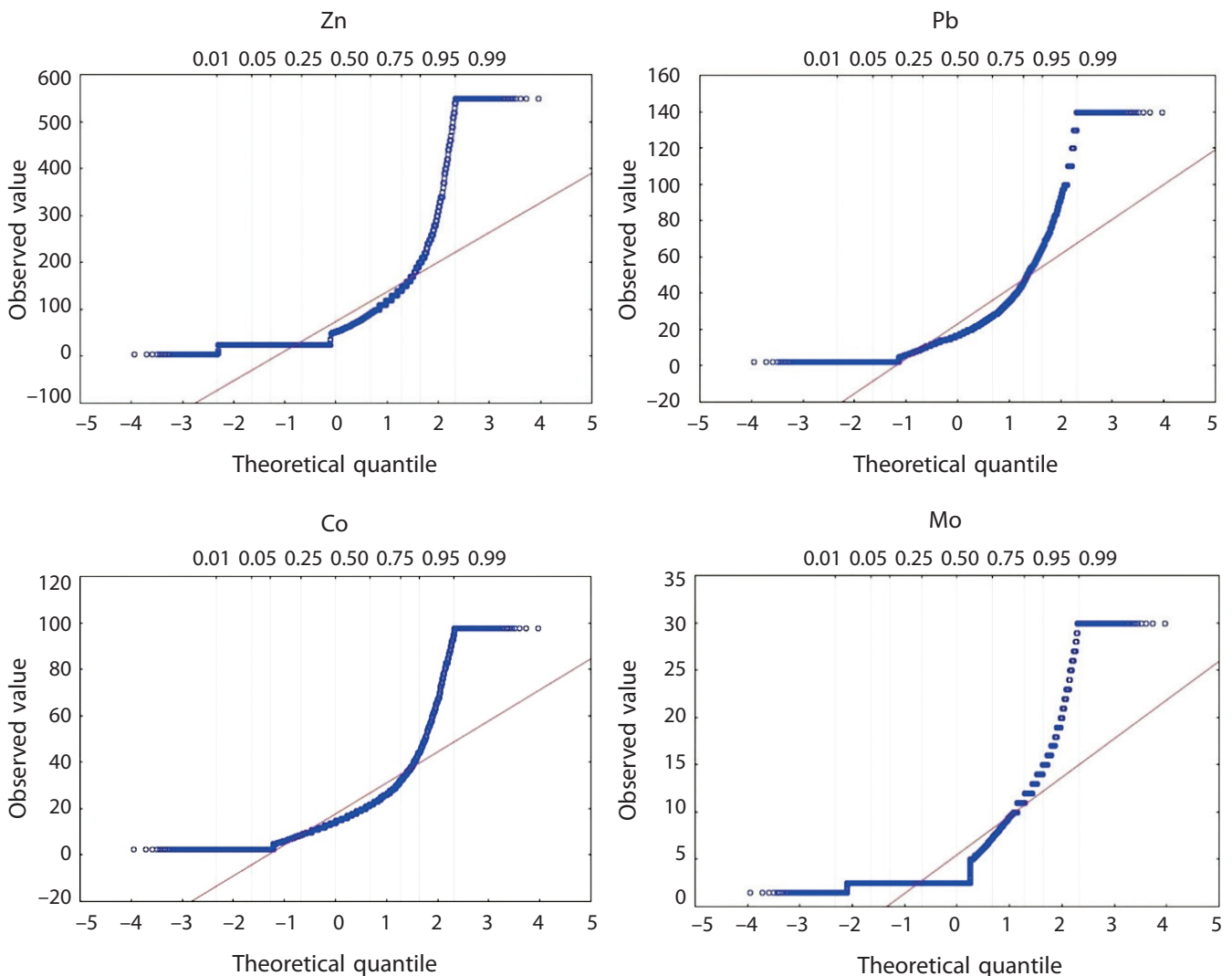


Рис. 12. Графики квантиль-квантиль логарифмически преобразованных данных по основным элементам в разрезе

Geochemical characteristics of trace elements in different lithologies in the Geokhimicheskoe ore occurrence

Таблица 1. Геохимические характеристики микроэлементов в различных литологиях на рудопоявлении Геохимическое

Lithology		Au	As	Sb	Ag	Ga	Cu	Co	Mo	Bi	Pb	Cr	P
All samples n = 620	Clarke of concentration	1266.67	300.00	51.00	6.80	3.00	5.95	7.00	12.00	2.27	8.24	4.09	18.29
	CV	3.97	3.95	2.05	0.65	0.59	0.78	0.86	0.91	0.19	0.98	0.76	1.66
	STD DEV	0.49	987.78	69.00	0.19	10.15	39.06	15.41	4.99	0.58	22.42	103.73	2152.97
	MEAN	0.12	250.22	33.72	0.29	17.14	49.79	17.84	5.50	3.11	22.92	135.78	1295.12
Standstones n = 24	Clarke of concentration	17.00	9.17	4.80	1.00	1.81	2.93	7.00	6.40	1.00	4.59	1.78	3.88
	CV	7.06	1.43	0.64	0.00	0.31	0.48	0.71	0.79	0.00	0.68	0.38	0.63
	STD DEV	0.06	52.12	7.38	0.00	5.29	22.97	11.77	4.41	0.00	13.81	82.32	563.17
	MEAN	0.01	36.51	11.49	0.25	16.93	47.37	16.63	5.61	3.00	20.17	219.39	891.31
Slates n = 41	Clarke of concentration	950.00	28.57	25.00	2.20	2.05	5.81	5.76	12.00	1.00	7.78	2.06	9.66
	CV	3.43	2.08	1.62	0.15	0.37	0.75	0.77	0.92	0.00	0.91	0.54	1.32
	STD DEV	0.53	198.64	44.73	0.04	6.90	41.25	16.28	5.83	0.00	22.36	97.55	1274.87
	MEAN	0.15	95.70	27.66	0.25	18.59	54.90	21.17	6.34	3.00	24.44	179.37	967.72
Siltstones n = 205	Clarke of concentration	422.22	158.14	19.62	6.80	2.83	4.81	6.53	5.36	2.27	7.37	3.15	13.64
	CV	3.37	3.42	1.71	0.80	0.55	0.70	0.94	0.85	0.25	0.89	0.67	1.52
	STD DEV	0.51	939.15	96.09	0.26	10.24	46.57	18.65	5.99	0.81	23.18	98.41	3093.48
	MEAN	0.15	274.95	56.18	0.33	18.65	66.94	19.94	7.08	3.21	25.96	146.75	2031.53
Granodiorites n = 238	Clarke of concentration	1100.00	390.00	16.00	3.56	2.67	4.17	4.50	7.60	1.00	7.50	4.09	6.33
	CV	4.34	3.96	2.06	0.49	0.57	0.67	0.71	0.86	0.10	0.97	0.76	1.26
	STD DEV	0.45	1042.41	38.78	0.13	9.82	27.46	11.78	3.63	0.30	21.29	103.52	1158.67
	MEAN	0.10	263.06	18.80	0.26	17.28	41.00	16.53	4.24	3.03	21.86	135.99	921.35
Limestone n = 46	Clarke of concentration	466.67	280.00	37.00	3.36	5.71	30.00	10.41	8.80	2.00	56.00	42.00	24.00
	CV	4.99	4.21	2.17	0.41	0.92	1.36	1.24	0.81	0.24	1.84	1.72	1.87
	STD DEV	0.25	280.19	65.22	0.11	4.24	30.77	13.89	4.53	0.77	23.26	39.78	1398.34
	MEAN	0.05	66.57	30.11	0.28	4.59	22.65	11.24	5.58	3.21	12.64	23.12	746.85
Siliceous siltstones n = 20	Clarke of concentration	214.29	42.31	13.00	2.12	3.30	5.64	7.00	7.20	2.00	5.00	5.19	50.00
	CV	4.65	4.77	1.02	0.21	0.57	0.79	1.05	0.76	0.10	0.75	0.81	2.43
	STD DEV	0.28	421.27	21.38	0.05	6.94	36.93	19.17	3.56	0.30	14.60	95.14	2288.34
	MEAN	0.06	88.31	21.06	0.26	12.25	46.71	18.33	4.70	3.03	19.36	117.93	940.31
Quartz vein n = 16	Clarke of concentration	633.33	503.23	51.00	6.80	5.15	8.93	6.29	12.00	2.27	5.71	8.12	18.33
	CV	2.32	2.26	2.46	0.77	0.81	1.09	0.90	0.99	0.26	1.01	1.18	1.44
	STD DEV	1.26	2592.13	59.25	0.27	10.41	42.18	9.36	5.07	0.82	37.10	79.29	830.03
	MEAN	0.54	1144.92	24.10	0.35	12.79	38.76	10.46	5.10	3.20	36.58	67.40	577.43
Diorites n = 30	Clarke of concentration	760.00	487.50	43.00	4.40	2.32	5.14	5.12	10.40	2.00	8.00	2.90	7.20
	CV	3.07	1.13	1.23	0.42	0.35	0.74	0.74	1.07	0.18	1.74	0.52	1.85
	STD DEV	1.01	2227.38	75.21	0.15	10.05	35.87	15.83	5.12	0.66	24.37	112.26	1235.47
	MEAN	0.38	903.74	46.14	0.28	23.76	46.37	21.53	5.26	3.14	23.59	177.25	1060.68

to particular rock types, suggesting that both primary depositional controls and subsequent remobilization processes influenced the current distribution of ore and pathfinder elements. The observed metal partitioning between different lithological units provides critical insights for understanding mineralization controls and developing targeted exploration strategies in analogous geological settings. The sandstone-hosted gold enrichment coupled with arsenic association in fine-grained siliceous rocks and antimony prevalence in vein systems collectively indicate potential epithermal or orogenic mineralization processes operating within the study area.

Elemental association

Certain elements can serve as valuable pathfinders for mineral deposit exploration due to their spatial association with specific mineralization types, while others may reflect unrelated geological processes or events. The obtained results reveal that gold, which relates to the primary component of interest, demonstrates weak correlations with typical siderophile group elements — with the notable exception of tungsten. However, it represents a relatively strong correlation with arsenic, a characteristic chalcophile element (figs. 13, 14). This unexpected geochemical relationship suggests that gold mineralization in the studied area may be more closely linked to hydrothermal processes involving arsenic-rich fluids rather than conventional magmatic or crustal differentiation trends typically related to siderophile elements. The observed elemental associations provide critical insights for refining exploration targeting criteria, particularly in distinguishing between different mineralization styles

and identifying potential vectors toward high-grade zones. The distinct correlation patterns between gold and arsenic, contrasting with its weaker affinity to traditional siderophile companions, underscore the complex geochemical behavior of gold under varying physicochemical conditions and emphasize the need for deposit-specific pathfinder element selection in exploration programs. These findings align with previous studies documenting similar gold-arsenic associations in epithermal and orogenic gold systems, where arsenic often serves as a key indicator of gold-bearing fluid pathways and depositional environments. The recognition of such diagnostic element pairs enhances the predictive capability of geochemical surveys and contributes to more efficient mineral resource assessment strategies in analogous geological terrains.

To establish the elemental associations related to mineralization processes, there was performed an R-mode factor analysis that extracted the principal component to derive independent components explaining the majority of dataset variances. The varimax rotation algorithm was subsequently applied to the factor loading matrix in order to optimize the interpretability by reducing cross-loadings between variables. A multidimensional scatter-plot representation (fig. 15) visualized a complete set of the analyzed variables. The dimensionality reduction process retained four principal components, with eigenvalues exceeding the Kaiser criterion threshold of 1.0, collectively accounting for 54.2 % of the total variance within the geochemical dataset. This analytical approach effectively delineated distinct elemental groupings that reflect different mineralization processes and paragenetic associations, with the rotated factor solution providing enhanced clarity in identifying key element clusters. The extracted

	Au	W	Ni	Cu	Co	As	Sb	Mo	Ag	Pb	Zn	Be	Mn	P
Au	100	52	7	12	7	77	13	12	8	11	5	3	4	1
W	52	100	14	29	16	53	30	21	48	20	17	16	3	7
Ni	7	14	100	60	61	6	24	24	8	20	55	2	7	22
Cu	12	29	60	100	54	11	39	32	29	26	44	9	12	35
Co	7	16	61	54	100	4	16	17	9	18	36	16	25	10
As	77	53	6	11	4	100	13	14	5	15	6	0	8	3
Sb	13	30	24	39	16	13	100	30	22	25	34	13	5	26
Mo	12	21	24	32	17	14	30	100	19	29	28	-1	13	25
Ag	8	48	8	29	9	5	22	19	100	17	20	21	3	15
Pb	11	20	20	26	18	15	25	29	17	100	33	2	4	14
Zn	5	17	55	44	36	6	34	28	20	33	100	6	20	26
Be	3	16	2	9	16	0	13	-1	21	2	6	100	6	6
Mn	4	3	7	12	25	8	5	13	3	4	20	6	100	7
P	1	7	22	35	10	3	26	25	15	14	26	6	7	100

Fig. 13. Correlation coefficient matrix of chemical elements by masses (%)

Рис. 13. Матрица коэффициентов корреляции химических элементов по массивам (%)

components demonstrate statistically significant associations between particular suites of elements, which offer valuable insights into the underlying geochemical processes governing metal distribution patterns. The cumulative explained variance percent-

age indicates that these four principal components capture the most essential relationships within the multivariate dataset while maintaining analytical parsimony. The resulting factor model serves as a robust foundation for interpreting the complex geochemical

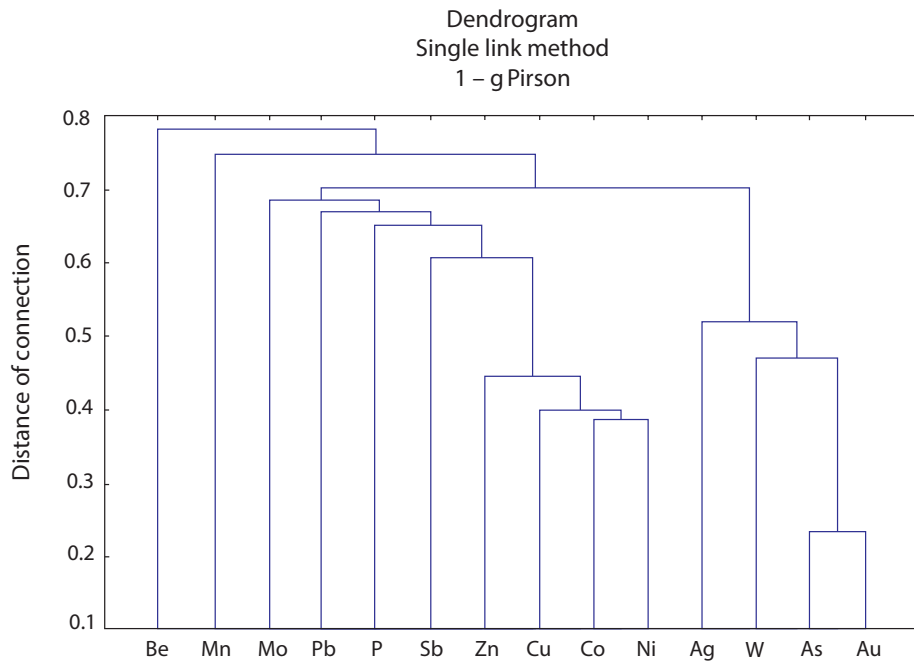


Fig. 14. Dendrogram of chemical elements relationships by masses

Рис. 14. Дендрограмма связей химических элементов по массивам

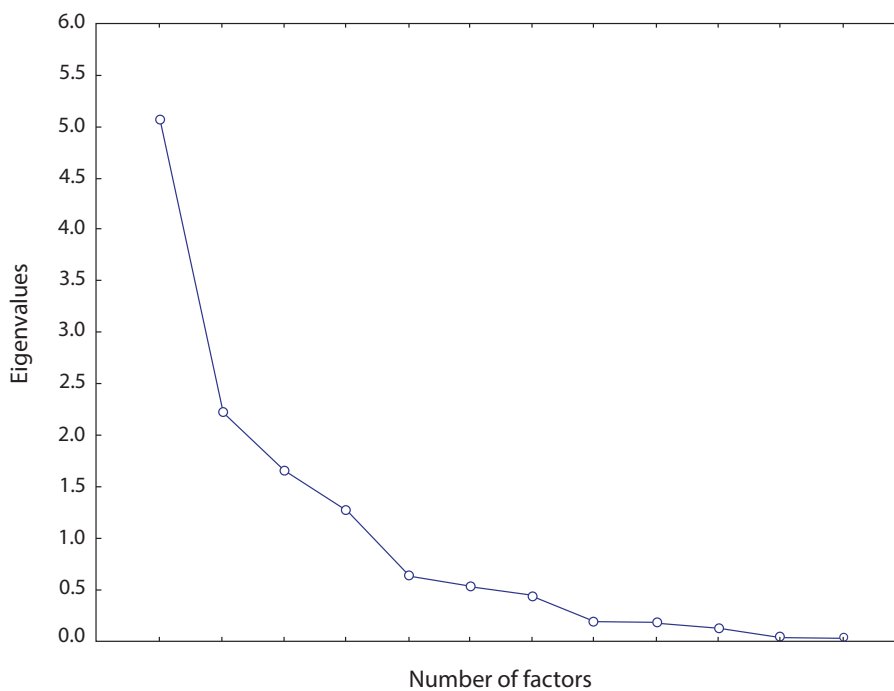


Fig. 15. Breakpoint line for factor analysis (after varimax rotation)

Рис. 15. Линия облома для факторного анализа (после варимакс-вращения)

signatures observed in the study area and establishing meaningful connections between elemental associations and specific mineralization events.

Table 2 comprehensively displays the factor analysis results and demonstrates how communality values quantify the proportion of each element's variance explained by the extracted factors, with elevated values signifying a more robust variable representation. The rotated component matrix revealed four distinct geochemical signatures: F1 exhibited strong loadings from a polymetallic association comprising W-Ga-Ni-Cu-Co-Sb-Bi-Cd-Zn-V-Li-Ge, suggesting a potential magmatic-hydrothermal origin. F2 represented preferential enrichment of Bi-Cd-Li, possibly indicating late-stage hydrothermal processes or secondary remobilization events. F3 demonstrated a characteristic Au-As pairing, typical of orogenic gold systems where arsenic serves as a pathfinder for gold mineralization. F4 was characterized by Co-Mn co-variation, potentially reflecting

redox-controlled deposition in specific lithological units. The differential element clustering across factors implies multiple superimposed mineralization events or varying physical and chemical conditions during ore formation. Particularly noteworthy is the segregation of gold and arsenic into a separate factor from base metals, reinforcing their distinct geochemical behavior and transport mechanisms. The high communality values for most elements confirm the model's effectiveness in capturing essential geochemical relationships, with certain elements demonstrating cross-loadings that may indicate transitional geochemical affinities or multiple genetic associations. These factor-derived elemental groupings provide a quantitative framework for understanding metal distribution patterns and developing targeted exploration strategies in similar geological environments.

The geochemical factor analysis revealed four distinct elemental groupings with specific geological

Table 2

Factor analysis loadings for all 22 analyzed elements (after varimax rotation)

Таблица 2. Нагрузки факторного анализа, выполненного для всех 22 анализируемых элементов (после варимакс-вращения)

Elements	Factor 1	Factor 2	Factor 3	Factor 4
Au	0.313	-0.067	0.724	-0.125
W	0.588	-0.274	0.469	-0.032
Ga	0.588	0.393	0.255	0.134
Ni	0.614	0.496	-0.252	-0.216
Cu	0.676	0.199	-0.277	-0.062
Co	0.502	0.375	-0.222	-0.506
As	0.318	-0.042	0.751	-0.082
Sb	0.516	-0.117	-0.159	0.256
Mo	0.450	0.040	-0.104	0.304
Ag	0.439	-0.415	-0.082	0.075
Bi	0.564	-0.649	-0.110	-0.046
Cd	0.576	-0.626	-0.180	-0.063
Pb	0.500	0.086	0.088	0.377
Zn	0.604	0.165	-0.313	-0.023
V	0.607	0.449	-0.099	0.141
Cr	0.366	0.525	0.225	-0.172
Sn	0.443	0.122	0.340	0.081
Be	0.205	-0.356	-0.109	-0.319
Li	0.553	-0.535	-0.127	-0.110
Ge	0.664	-0.059	0.099	0.103
Mn	0.187	0.004	-0.084	-0.511
P	0.314	0.110	-0.291	0.363
Explained variance	5.524	2.617	2.062	1.233
Probability of total variance contribution (%)	25.1	11.9	9.4	5.6

implications. The F1 cluster predominantly comprised siderophile elements (W-Ga-Ni-Cu-Co-Sb-Bi-Cd-Zn-V-Li-Ge) typically found in olivine and pyroxene minerals, exhibiting strong association with limestone and quartz vein systems in the Geokhimicheskoe ore occurrence. This assemblage suggests primary magmatic differentiation processes. The F2 grouping (Bi-Cd-Li) exhibits characteristics of high-temperature hydrothermal metasomatism, displaying genetic links to granite-related mineralization events. Of particular metallogenic significance, the F3 association (Au-As) represents a diagnostic element pair for gold mineralization, with its chalcophile affinity indicating deposition under intermediate-to-low temperature conditions within a gold-arsenopyrite-quartz mineralizing stage — this factor effectively delineates the primary ore-forming event and identifies secondary dispersion halos around gold-bearing structures. The final F4 grouping (Co-Mn) reflects precipitation of these elements as sulfides or carbonates in hydrothermal systems, with manganese occurring in rhodochrosite (MnCO_3) and cobalt in cobaltite (CoAsS) or carrollite (CuCo_2S_4), characteristic of moderate-to-low temperature vein-type mineralization.

Geochemical halos of gold and associated pathfinder elements

Factor analysis differentiated mixed geochemical populations and detected anomalies within the initial

factor scores. The Surfer® 18.1.186 software (advanced contouring, gridding, and 3D surface mapping application) generated visual representations, including point data interpolation into raster maps, primary geochemical halo delineation, additive indicator localization plans on primary dispersion halos, and multiplicative indicator distribution mapping.

The resulting anomaly maps (figs. 16–22) display a clear separation between background and anomalous values, with gold assay sample locations (marked by black triangles in fig. 21) intersecting known mineralized zones. The background values exhibit heterogeneous distribution across the study area, with sampling points occurring in both high- and low-background regions. This irregular pattern demonstrates limitations to conventional anomaly identification techniques based solely on mean and standard deviation calculations relating to non-uniform background distributions.

Areas with elevated background concentrations exhibit strong spatial correlation with altered sandstones and granite dikes, suggesting their potential role as metal sources for ore formation processes. Anomaly morphology analysis (figs. 16–22) reveals distinct structural control by a plastic shear zone. The fractal-attractor analytical method proved to be particularly effective in enhancing subtle geochemical anomalies, with the majority of samples demonstrating significant assay results clustered within or adjacent to high-anomaly zones. Minor discrepancies should

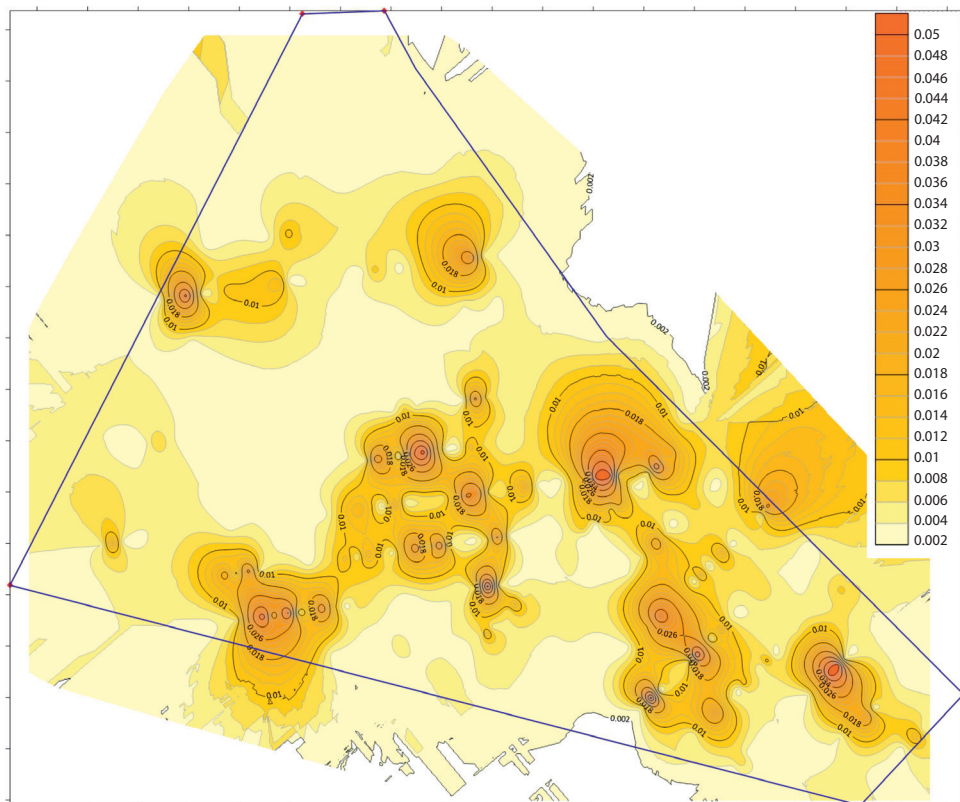


Fig. 16. Primary geochemical halos of Au in the Geokhimicheskoe ore occurrence

Рис. 16. Первичные геохимические ореолы Au на рудопроявлении Геохимическое

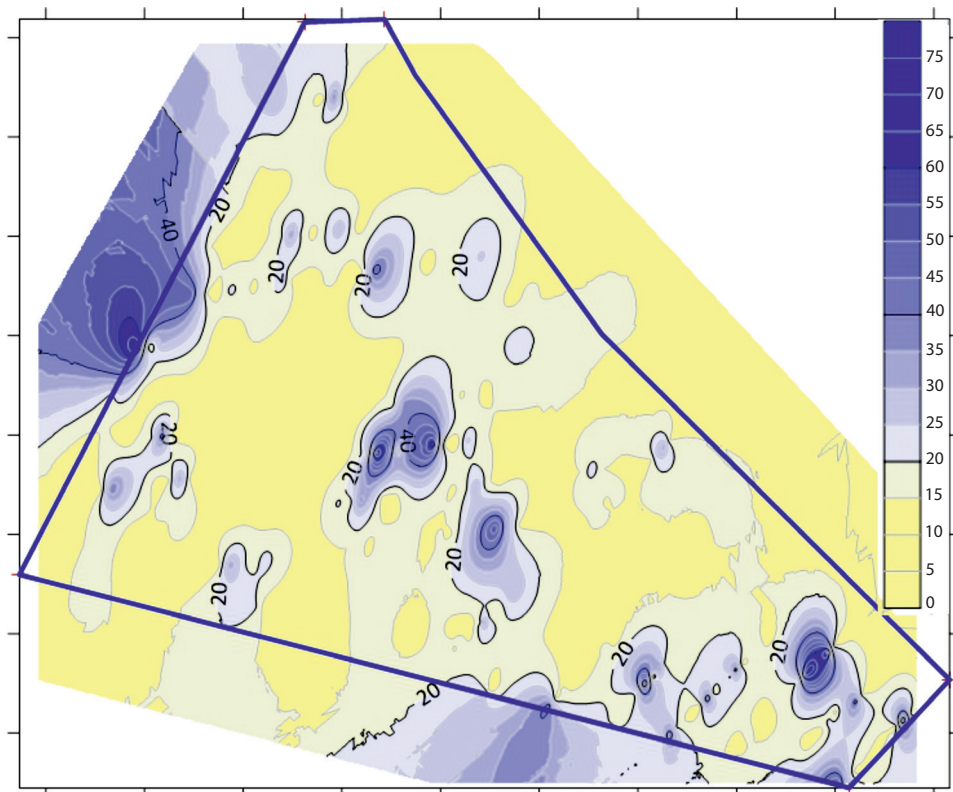


Fig. 17. Primary geochemical halos of As in the Geokhimicheskoe ore occurrence

Рис. 17. Первичные геохимические ореолы As на рудопроявлении Геохимическое

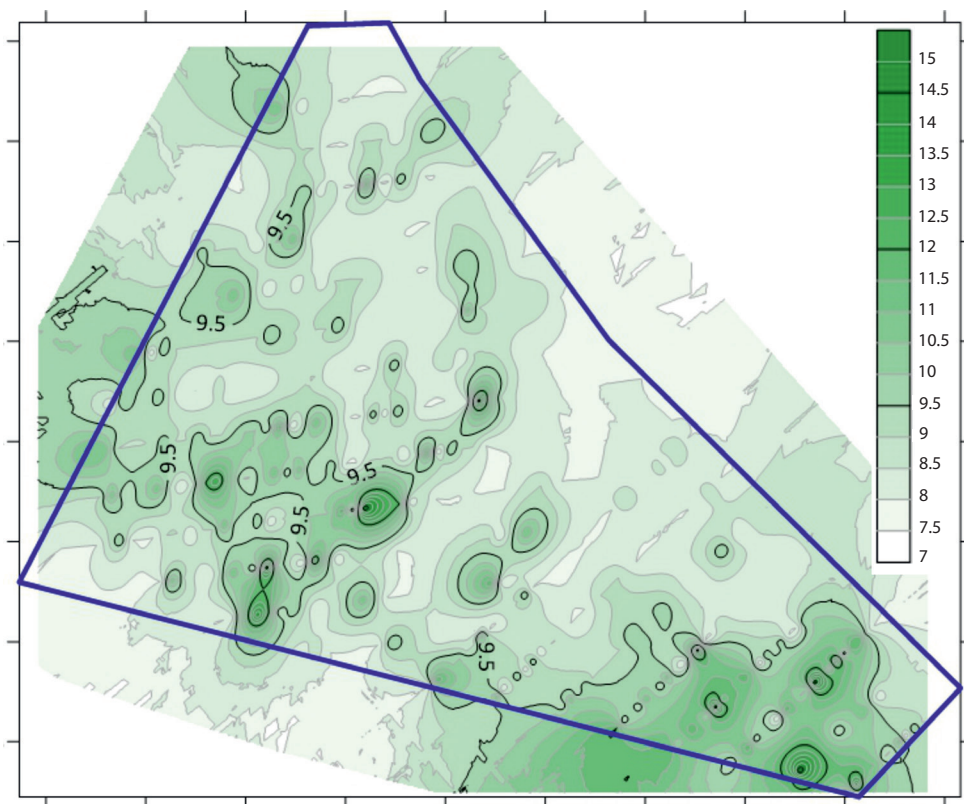


Fig. 18. Primary geochemical halos of Co in the Geokhimicheskoe ore occurrence

Рис. 18. Первичные геохимические ореолы Co на рудопроявлении Геохимическое

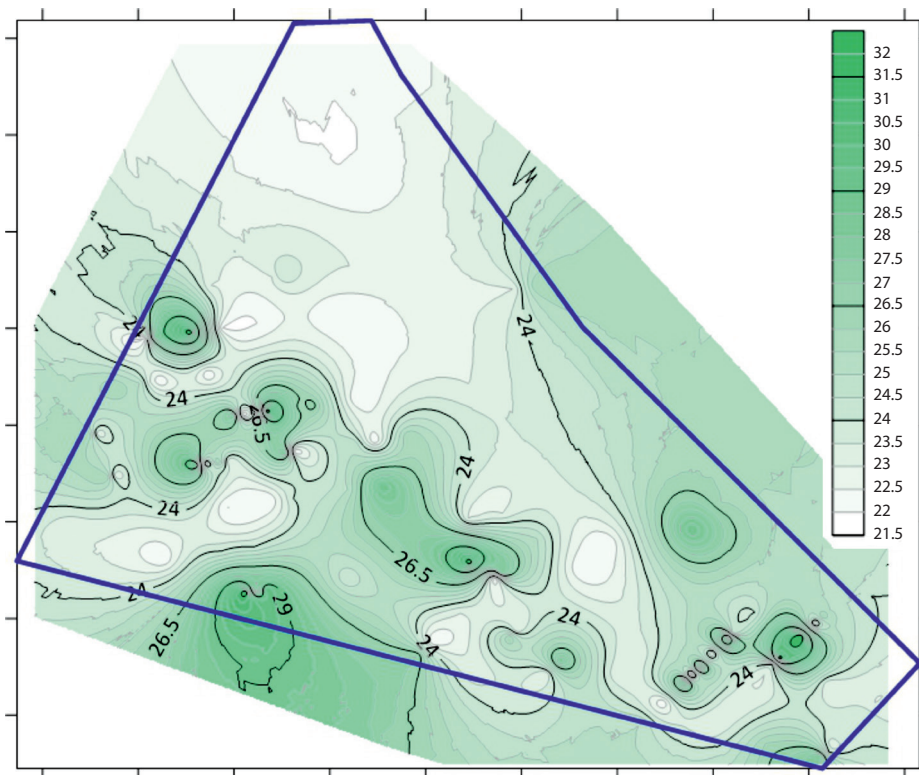


Fig. 19. Primary geochemical halos of Cu in the Geokhimicheskoe ore occurrence

Рис. 19. Первичные геохимические ореолы Cu на рудопроявлении Геохимическое

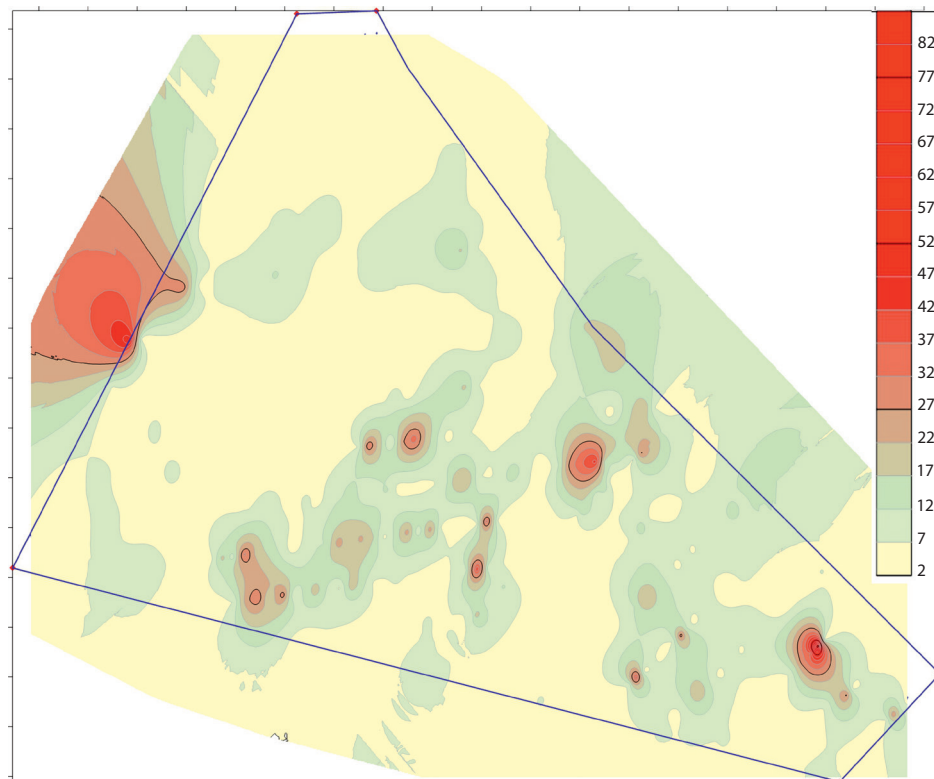


Fig. 20. Localization map of additive indicators (Au-As) on primary geochemical dispersion halos in the Geokhimicheskoe ore occurrence

Рис. 20. План локализации аддитивных индикаторов (Au-As) на первичных геохимических ореолах рассеяния на рудопроявлении Геохимическое

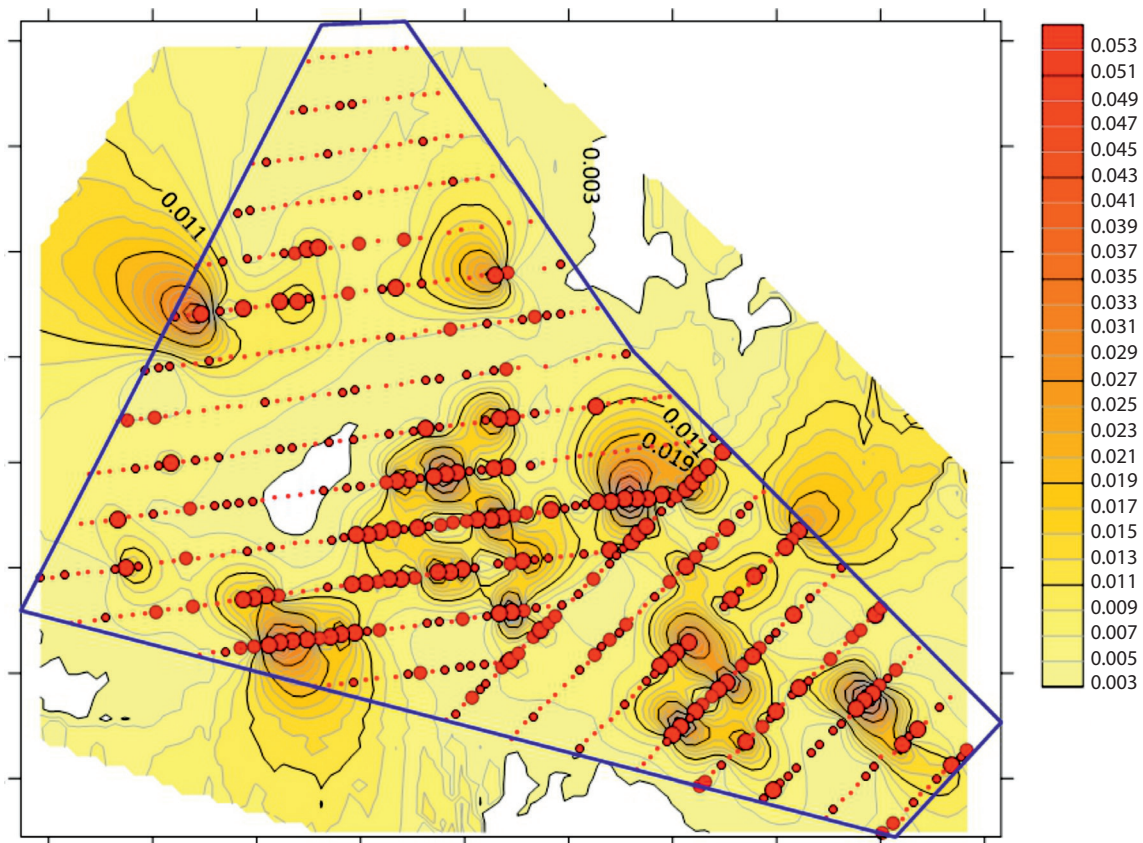


Fig. 21. Primary geochemical halos of Au in the Geokhimicheskoe ore occurrence, with sampling points located
The figure size varies depending on the Au indicator

Рис. 21. Первичные геохимические ореолы Au на рудопоявлении Геохимическое с точками опробования
Размер фигуры варьируется в зависимости от индикатора Au

reflect sampling inconsistencies, which further validate the predictive capability of the fractal-attractor method in this geological environment and its effectiveness in identifying promising exploration targets for subsequent investigation. The integrated approach, which combines factor analysis with advanced spatial interpretation techniques, provides a robust framework for understanding complex element dispersion patterns and optimizing mineral exploration strategies in similar geological settings.

CONCLUSION

The study conducted in the Geokhimicheskoe gold occurrence demonstrated effectiveness of geochemical exploration methods to identify anomalies associated with gold mineralization. Factor analysis detected polymetallic element associations that can serve as direct indicators for ore prospecting, yielding the following key findings.

The applied factor analysis model revealed that gold-related polymetallic elements in the Geokhimicheskoe ore occurrence include As and W. The factor distribution patterns also highlighted geochemical zonation, which indicated that gold mineralization is preferentially localized in metasedimentary sandstones

influenced by mineralizing fluids derived from granitic dikes and concentrated along northwest-southeast trending fault zones.

Within the Geokhimicheskoe ore occurrence in the Kuldzhuktau Mountains, there were identified the following rock types: quartzites, various schists, granitoids, diorites, dacites, quartz veins, breccias, etc. All rock units exhibited varying degrees of metasomatic alteration, with sericitization, iron oxidation, silicification, and carbonatization being the most widespread. Ore mineralization across all rock types is predominantly represented by iron and arsenic hydroxides, secondary copper minerals, and hematite, typically occurring as disseminated textures with occasional thin veinlets and ochreous fracture fillings.

Gold was identified as the principal economic component in the sampled material, with elevated concentrations detected in selected samples. Strong positive correlations were established between gold, arsenic, and tungsten contents, which attributed to the presence of gold-pyrite-arsenopyrite and gold-rare metal paragenetic mineral associations. Elevated arsenic and tungsten concentrations serve as reliable geochemical indicators for gold mineralization.

In terms of mineralogical and geochemical characteristics, the gold mineralization in the Geokhimicheskoe

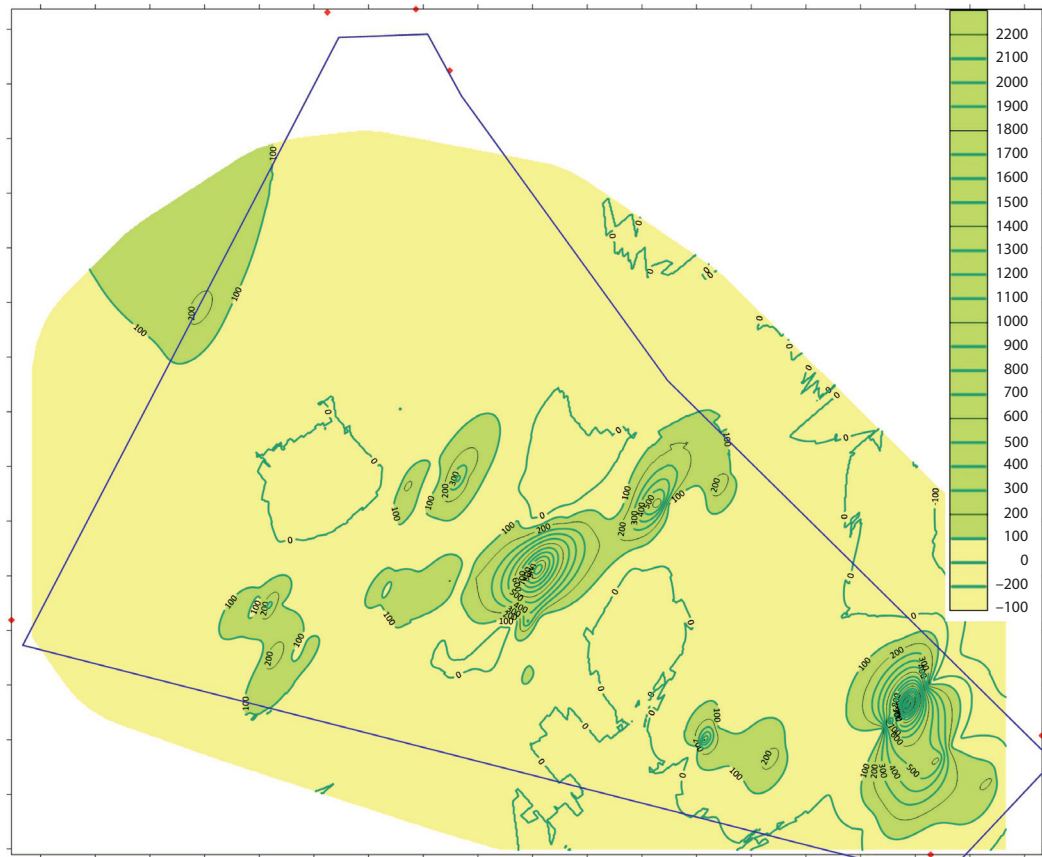


Fig. 22. Multiplicative indicator ($Au \times As$) distribution across the area in the Geokhimicheskoe ore occurrence

Рис. 22. Распределение мультипликативного индикатора ($Au \times As$) на площади рудопоявления Геохимическое

gold occurrence exhibits significant similarities to the Taushan ore deposits, suggesting comparable formation conditions and potential genetic relationships between these mineralized systems. The integrated application of factor analysis and geochemical mapping techniques has proven to be effective in distinguishing mineralization-related element associations from background distributions, providing a robust methodology for exploration in similar geological environments. The identified element correlations and spatial distribution patterns offer valuable criteria for future prospecting efforts in the region, particularly for concealed gold mineralization associated with arsenic and tungsten anomalies. These findings contribute to the development of more efficient exploration models for gold deposits in analogous metallogenic provinces.

REFERENCES

1. Bounessah M., Atkin B. P. An application of exploratory data analysis (EDA) as a robust non-parametric technique for geochemical mapping in a semi-arid climate. *Applied Geochemistry*. 2003; 18 (8): 1185–1195. [https://doi.org/10.1016/S0883-2927\(02\)00247-0](https://doi.org/10.1016/S0883-2927(02)00247-0).
2. Identification of weak anomalies: A multifractal perspective / R. Zuo [et al.]. *Journal of Geochemical Exploration*. 2015; 148: 12–24. <https://doi.org/10.1016/j.gexplo.2014.05.005>.
3. Zhmodik S. M., Roslyakova N. V. Geochemistry of gold in hydrothermal processes. *Development history of the Institute of Geology and Geophysics, Siberian Branch (AS USSR and RAS) and its research areas*. Novosibirsk: Acad. Publ. House "Geo"; 2010. P. 486–490. (In Russ.).
4. Kim J.-O., Mueller Ch. W. Factor analysis: Statistical methods and practical issues. *Factor, discriminant, and cluster analysis* / J.-O. Kim [et al.]; transl. A. M. Khotinskiy, S. B. Korolev; Ed. I. S. Enyukov. Moscow: Finances and Statistics; 1989. P. 5–77. (In Russ.).
5. Sinclair A. J. Selection of threshold values in geochemical data using probability graphs. *Journal of Geochemical Exploration*. 1974; 3 (2): 129–149. [https://doi.org/10.1016/0375-6742\(74\)90030-2](https://doi.org/10.1016/0375-6742(74)90030-2).
6. Stanley C. R., Sinclair A. J. Comparison of probability plots and the gap statistic in the selection of thresholds for exploration geochemistry data. *Journal of Geochemical Exploration*. 1989; 32 (1–3): 355–357. [https://doi.org/10.1016/0375-6742\(89\)90076-9](https://doi.org/10.1016/0375-6742(89)90076-9).
7. Kürzl H. Exploratory data analysis: Recent advances for the interpretation of geochemical data. *Journal of Geochemical Exploration*. 1988; 30 (1–3): 309–322. [https://doi.org/10.1016/0375-6742\(88\)90066-0](https://doi.org/10.1016/0375-6742(88)90066-0).
8. Reimann C. Geochemical mapping: Technique or art? *Geochemistry: Exploration, Environment, Analysis*. 2005; 5 (4): 359–370. <https://doi.org/10.1144/1467-7873/03-051>.
9. Chiprés J. A., Castro-Larragoitia J., Monroy M. G. Exploratory and spatial data analysis (EDA-SDA) for determining regional background levels and anomalies of potentially toxic elements in soils from Catorce-Matehuala, Mexico. *Applied Geochemistry*. 2009; 24 (8): 1579–1589. <https://doi.org/10.1016/j.apgeochem.2009.04.022>.

10. Zhao J., Chen S., Zuo R. Identifying geochemical anomalies associated with Au-Cu mineralization using multifractal and artificial neural network models in the Ningqiang district, Shaanxi, China. *Journal of Geochemical Exploration*. 2016; 164: 54–64. <https://doi.org/10.1016/j.gexplo.2015.06.018>.
11. Agterberg F. P. Multifractal simulation of geochemical map patterns. *Geologic modeling and simulation. Computer applications in the earth sciences* / Eds. D. F. Merriam, J. C. Davis. Boston, MA: Springer; 2001. P. 327–346. https://doi.org/10.1007/978-1-4615-1359-9_17.
12. Reimann C., Filzmoser P., Garrett R. G. Factor analysis applied to regional geochemical data: Problems and possibilities. *Applied Geochemistry*. 2002; 17 (3): 185–206. [https://doi.org/10.1016/S0883-2927\(01\)00066-X](https://doi.org/10.1016/S0883-2927(01)00066-X).
13. Razikov O. T., Maripova S. T., Tokhirzhonov K. O. Artificial intelligence methods in classifying geological and structural blocks with various metallogenic specialization in the mountains of Kuldzhuktau (Uzbekistan). *Proc. of Sci. Conf. "Current Issues of Prospecting Geology"*, Moscow, 22–24 Nov. 2022. Moscow: VIMS; 2023. P. 248–256. (In Russ.).
14. Khamrabaev I. Kh. Magmatism and postmagmatic processes in Western Uzbekistan. Tashkent: Uzbek SSR Acad. of Sci. Publ. House; 1956. 471 p. (In Russ.).
15. Karpova E. D. Metallogenic zoning of the Tien Shan and Pamirs. *Soviet Geology*. 1959; (8): 81–101. (In Russ.).
16. Geology of USSR. Vol. XXIII. Uzbek SSR. Mineral resources / Ed. Kh. T. Tulyaganov. Moscow: Nedra; 1983. 232 p. (In Russ.).
17. Borovikov V. P. Statistica. The art of computer-based data analysis. 2nd ed. Moscow [et al.]: Piter; 2003. 688 p. (In Russ.).
18. Belonin M. D., Golubeva V. A., Skublov G. T. Factor analysis in geology. Moscow: Nedra; 1982. 269 p. (In Russ.).
19. Kaiser H. F. An index of factorial simplicity. *Psychometrika*. 1974; 39 (1): 31–36. <https://doi.org/10.1007/BF02291575>.
20. Deposit density of tungsten polymetallic deposits in the eastern Nanling metallogenic belt, China / T. Li [et al.]. *Ore Geology Reviews*. 2018; 94: 73–92. <https://doi.org/10.1016/j.oregeorev.2018.01.010>.
21. Bartlett M. S. Tests of significance in factor analysis. *British Journal of Statistical Psychology*. 1950; 3 (2): 77–85. <https://doi.org/10.1111/j.2044-8317.1950.tb00285.x>.
5. Sinclair A. J. Selection of threshold values in geochemical data using probability graphs // *Journal of Geochemical Exploration*. 1974. Vol. 3, no. 2. P. 129–149. [https://doi.org/10.1016/0375-6742\(74\)90030-2](https://doi.org/10.1016/0375-6742(74)90030-2).
6. Stanley C. R., Sinclair A. J. Comparison of probability plots and the gap statistic in the selection of thresholds for exploration geochemistry data // *Journal of Geochemical Exploration*. 1989. Vol. 32, nos. 1–3. P. 355–357. [https://doi.org/10.1016/0375-6742\(89\)90076-9](https://doi.org/10.1016/0375-6742(89)90076-9).
7. Kürzl H. Exploratory data analysis: Recent advances for the interpretation of geochemical data // *Journal of Geochemical Exploration*. 1988. Vol. 30, nos. 1–3. P. 309–322. [https://doi.org/10.1016/0375-6742\(88\)90066-0](https://doi.org/10.1016/0375-6742(88)90066-0).
8. Reimann C. Geochemical mapping: Technique or art? // *Geochemistry: Exploration, Environment, Analysis*. 2005. Vol. 5, no. 4. P. 359–370. <https://doi.org/10.1144/1467-7873/03-051>.
9. Chiprés J. A., Castro-Larragoitia J., Monroy M. G. Exploratory and spatial data analysis (EDA-SDA) for determining regional background levels and anomalies of potentially toxic elements in soils from Catorce-Matehuala, Mexico // *Applied Geochemistry*. 2009. Vol. 24, no. 8. P. 1579–1589. <https://doi.org/10.1016/j.apgeochem.2009.04.022>.
10. Zhao J., Chen S., Zuo R. Identifying geochemical anomalies associated with Au-Cu mineralization using multifractal and artificial neural network models in the Ningqiang district, Shaanxi, China // *Journal of Geochemical Exploration*. 2016. Vol. 164. P. 54–64. <https://doi.org/10.1016/j.gexplo.2015.06.018>.
11. Agterberg F. P. Multifractal simulation of geochemical map patterns // *Geologic modeling and simulation. Computer applications in the earth sciences* / Eds. D. F. Merriam, J. C. Davis. Boston, MA : Springer, 2001. P. 327–346. https://doi.org/10.1007/978-1-4615-1359-9_17.
12. Reimann C., Filzmoser P., Garrett R. G. Factor analysis applied to regional geochemical data: Problems and possibilities // *Applied Geochemistry*. 2002. Vol. 17, no. 3. P. 185–206. [https://doi.org/10.1016/S0883-2927\(01\)00066-X](https://doi.org/10.1016/S0883-2927(01)00066-X).
13. Разиков О. Т., Марипова С. Т., Тохиржонов К. О. Применение методов искусственного интеллекта в классификации геолого-структурных блоков с различной металлогенической специализацией в горах Кульджуқтау (Узбекистан) // Тр. науч.-практ. конф. «Актуальные проблемы поисковой геологии», Москва, 22–24 нояб. 2022 г. М. : ФГБУ «ВИМС», 2023. С. 248–256.
14. Хамрабаев И. Х. Магматизм и постмагматические процессы в Западном Узбекистане. Ташкент : Изд-во Акад. наук УзССР, 1958. 471 с.
15. Карпова Е. Д. Металлогеническое районирование Тянь-Шаня и Памира // *Советская геология*. 1959. № 8. С. 81–101.
16. Геология СССР. Т. XXIII. Узбекская ССР. Полезные ископаемые / Под ред. Х. Т. Туляганова. М. : Недра, 1983. 232 с.
17. Боровиков В. П. Statistica. Искусство анализа данных на компьютере. 2-е изд. М. [и др.] : Питер, 2003. 688 с.
18. Белонин М. Д., Голубева В. А., Скублов Г. Т. Факторный анализ в геологии. М. : Недра, 1982. 269 с.
19. Kaiser H. F. An index of factorial simplicity // *Psychometrika*. 1974. Vol. 39, no. 1. P. 31–36. <https://doi.org/10.1007/BF02291575>.
20. Deposit density of tungsten polymetallic deposits in the eastern Nanling metallogenic belt, China / T. Li [et al.] // *Ore Geology Reviews*. 2018. Vol. 94. P. 73–92. <https://doi.org/10.1016/j.oregeorev.2018.01.010>.
21. Bartlett M. S. Tests of significance in factor analysis // *British Journal of Statistical Psychology*. 1950. Vol. 3, no. 2. P. 77–85. <https://doi.org/10.1111/j.2044-8317.1950.tb00285.x>.

СПИСОК ИСТОЧНИКОВ

1. Bounessah M., Atkin B. P. An application of exploratory data analysis (EDA) as a robust non-parametric technique for geochemical mapping in a semi-arid climate // *Applied Geochemistry*. 2003. Vol. 18, no. 8. P. 1185–1195. [https://doi.org/10.1016/S0883-2927\(02\)00247-0](https://doi.org/10.1016/S0883-2927(02)00247-0).
2. Identification of weak anomalies: A multifractal perspective / R. Zuo [et al.] // *Journal of Geochemical Exploration*. 2015. Vol. 148. P. 12–24. <https://doi.org/10.1016/j.gexplo.2014.05.005>.
3. Жмодик С. М., Рослякова Н. В. Геохимия золота в гидротермальных процессах // История развития Института геологии и геофизики СО (АН СССР и РАН) и его научных направлений. Новосибирск : Акад. изд-во «Гео», 2010. С. 486–490.
4. Ким Дж.-О., Мьюллер Ч. У. Факторный анализ: статистические методы и практические вопросы // Факторный, дискриминантный и кластерный анализ / Дж.-О. Ким [и др.] ; пер. с англ. А. М. Хотинского, С. Б. Королева ; под ред. И. С. Енюкова. М. : Финансы и статистика, 1989. С. 5–77.

Bekhruz B. Oganiyozov

MSc (Earth Sciences), Independent Researcher (PhD)

University of Geological Sciences,
Tashkent, Uzbekistan

<https://orcid.org/0009-0004-0849-9536>
behruzoga@gmail.com

Majid M. Pirnazarov

DSc (Geology and Mineralogy),
Senior Researcher,
Vice-Rector for Educational and Spiritual Affairs

University of Geological Sciences,
Tashkent, Uzbekistan

m.pirnazarov@uzgeouniver.uz

Бехруз Б. Оганиёзов

Магистр наук о Земле, независимый исследователь (PhD)

Университет геологических наук Республики Узбекистан,
Ташкент, Узбекистан

<https://orcid.org/0009-0004-0849-9536>
behruzoga@gmail.com

Маджид М. Пирназаров

Доктор геолого-минералогических наук,
старший научный сотрудник,
проректор по учебно-воспитательной работе

Университет геологических наук Республики Узбекистан,
Ташкент, Узбекистан

m.pirnazarov@uzgeouniver.uz

Contribution of the authors: the authors contributed equally to this article.

Conflict of interest: the authors declare no conflicts of interest.

Вклад авторов: все авторы сделали эквивалентный вклад в подготовку публикации.

Конфликт интересов: авторы заявляют об отсутствии конфликта интересов.

Статья поступила в редакцию 27.02.2025
Одобрена после рецензирования 25.04.2025
Принята к публикации 20.06.2025

Submitted 27.02.2025
Approved after reviewing 25.04.2025
Accepted for publication 20.06.2025